PHYSICAL REVIEW D VOLUME 18, NUMBER 11 1 DECEMBER 1978

P-wave baryons in the quark model

Nathan Isgur*
Department of Physics, University of Toronto, Toronto, Canada

Gabriel Karl
Department of Physics, University of Guelph, Guelph, Canada
(Received 10 February 1978; revised manuscript received 6 September 1978)

We discuss the spectrum and mixing angles of negative-parity baryons in a quark-model framework inspired by quantum chromodynamics. We take into account in zero order the removal of the degeneracy between the two P-wave states of the three-quark system in the $S = -1$ sector, as well as the hyperfine interaction between quarks, but neglect spin-orbit coupling. We find good agreement with experiment in the $S = 0$ and $S = -1$ sectors where there are data and predict the $S = -2, -3$ sectors.

I. INTRODUCTION

The experimental discovery of the J/ψ and related particles has given strong moral support to theoretical work on quark models. Much recent work has been inspired by concrete proposals[1] for quark-quark interactions based on the analogy between chromodynamics and ordinary electrodynamics.

We are concerned here with the masses and mixings of low-lying negative-parity baryons in a quark-model framework. We are guided by ideas widely expected to hold true in chromodynamics: a universal confining interaction potential—the same for all flavors (masses) and spin orientations of quark—and a hyperfine interaction between quarks along the lines of a recent proposal.[1a] These guidelines are sufficient to understand the large body of data available on these states in a simple way.

Although many of our conclusions are quite general, we shall at first discuss a very simple harmonic-oscillator model where our assertions are (we hope) very transparent and well defined. The assumptions made about the interactions between quarks are spelled out in Sec. II: We take only harmonic springs and hyperfine interactions. Our task is then extremely simple in principle: We have to diagonalize the interaction in the relevant space of states—the negative-parity baryons. This involves choosing carefully zero-order wave functions. While our choice is quite traditional for those states which are composed of equal-mass quarks ($S = 0$ and $S = -3$ sector), the zero-order wave functions chosen for the other states ($S = -1$, -2 sectors) are somewhat novel. The usual prescription[2] is to symmetrize between all three quarks. We only symmetrize between equal-mass (up and down) quarks. This is discussed in Sec. III.

We then compare the most naive version of the model we investigate with experiment. In our first report on this work[3] we discussed the nonstrange sector and found good agreement between the naive model and the data. We therefore concentrate in Sec. IV on the $S = -1$ sector (Λ's and Σ's) where a large quantity of data is available.[10] We find again good agreement with experiment where data exist. As a result we feel that there is little risk in predicting the $S = -2$ and -3 sectors where there are almost no data.

In Secs. V and VI we go beyond the simple assumptions made in the initial discussion: the restriction to harmonic-oscillator states (which is easy to relax), and the neglect of spin-orbit coupling. We find the data indicate that harmonic oscillators are a good choice of wave function and that not much spin-orbit coupling is required. We also discuss possible reasons for the absence of spin-orbit coupling. Our discussion here has much overlap with recent work on charmonium where similar conclusions have been reached.[4,5]

The negative-parity baryons have been discussed in a quark-model framework in the work of Greenberg,[6] Dalitz,[7] and their collaborators. The approximation followed in this early work consisted in neglecting tensor forces and keeping instead spin-orbit coupling. This approximation is orthogonal to the prescription suggested by quantum chromodynamics (QCD) which we use. While the experimental mass spectrum can be reproduced in this way, the observed mixing angles are a problem. More recently, since the original application[1a] of the Fermi-Breit Hamiltonian to quarks, negative-parity baryons have been discussed by Celmaster[8] and by Gromes and Stamatescu.[9] We differ from both these references in our deliberate neglect of spin-orbit coupling, and our choice of zero-order wave functions. Celmaster keeps the full spin-orbit coupling present in the Breit Hamiltonian, but neglects spin-orbit coupling coming

from the confinement potential. As a consequence he predicts the lowest-mass nonstrange negative-parity baryon at about 1330 MeV instead of the experimentally observed lowest-mass state at 1520 MeV. In our opinion this demonstrates clearly that spin-orbit coupling is just not present at the level predicted by the Breit Hamiltonian.[9] The initial work of Gromes and Stamatescu[9] neglects the tensor part of the Breit interaction; this restriction is removed in subsequent work by Gromes. These authors discuss only $S=0$ states.

II. ZERO-ORDER MODEL: HARMONIC OSCILLATORS + HYPERFINE COUPLING

We repeat that this model is discussed primarily for the reader's convenience; generalizations and comments are relegated to Secs. V, VI, and VII.

We assume throughout that the splitting of the family of negative-parity baryons is preponderantly due to the hyperfine interaction $H_{\rm hyp}$ between each pair of quarks (i,j) of the form[1a]

$$H_{\rm hyp}^{ij}=\frac{2\alpha_s}{3m_im_j}\left[\frac{8\pi}{3}\delta^3(\vec{r}_{ij})\vec{S}_i\cdot\vec{S}_j+\frac{1}{r_{ij}^3}(3\vec{S}_i\cdot\hat{r}_{ij}\vec{S}_j\cdot\hat{r}_{ij}-\vec{S}_i\cdot\vec{S}_j)\right], \quad (2.1)$$

where m_i and $\vec{S}_i$ are the mass and spin of the ith quark and $\vec{r}_{ij}$ is the separation between a pair of quarks. Aside from the overall constant in front, this is the familiar magnetic-dipole–magnetic-dipole component of the Breit Hamiltonian.[11] De Rújula *et al.* conjectured that the Breit Hamiltonian would apply to quark-quark interactions mediated by gluons, where α_s would be the quark-gluon fine-structure constant. We have discarded the spin-orbit part of their ansatz and view in what follows α_s as a free parameter.

The first term (which we denote by $H_{\rm contact}^{ij}$) is called the Fermi contact term, and operates only when the quark pair (ij) has zero orbital angular momentum while the second term ($H_{\rm tensor}^{ij}$), often called the tensor term, is operative only in states with nonzero orbital angular momentum between the quarks i and j.

The negative-parity baryons are especially suitable for studying the hyperfine interaction. These baryons belong in the quark model to a multiplet of 70 states with $L=1$. In the simplest models, which we assume here, this unit of orbital angular momentum resides in one of the two quark relative coordinates. Thus in one coordinate only the tensor term is operative while the contact term alone operates in the other. These baryons are therefore a good place to test simultaneously both pieces of the hyperfine interaction. The Hamiltonian responsible for the confining forces between three quarks 1, 2, and 3, of which quarks 1 and 2 have equal masses m while quark 3 has mass m' (this is the most general case required for the states of interest in this paper), is

$$H_{\rm HO}=\frac{p_1^2}{2m}+\frac{p_2^2}{2m}+\frac{p_3^2}{2m'}+\tfrac{1}{2}K|\vec{r}_1-\vec{r}_2|^2+\tfrac{1}{2}K|\vec{r}_1-\vec{r}_3|^2+\tfrac{1}{2}K|\vec{r}_2-\vec{r}_3|^2. \quad (2.2)$$

If we define

$$\vec{\rho}\equiv\frac{1}{\sqrt{2}}(\vec{r}_1-\vec{r}_2),$$
$$\vec{\lambda}\equiv\frac{1}{\sqrt{6}}(\vec{r}_1+\vec{r}_2-2\vec{r}_3), \quad (2.3)$$
$$\vec{R}_{\rm c.m.}\equiv\frac{m(\vec{r}_1+\vec{r}_2)+m'\vec{r}_3}{2m+m'},$$

then we obtain

$$H_{\rm HO}=\frac{p_{\rm cm}^2}{2M}+\frac{p_\rho^2}{2m_\rho}+\frac{p_\lambda^2}{2m_\lambda}+\tfrac{3}{2}K\rho^2+\tfrac{3}{2}K\lambda^2, \quad (2.4)$$

where

$$M=2m+m',\quad m_\rho\equiv m,\quad m_\lambda\equiv\frac{3mm'}{2m+m'}, \quad (2.5)$$

$$\vec{p}_{\rm c.m.}=M\frac{d\vec{R}_{\rm c.m.}}{dt},\quad \vec{p}_\rho=m_\rho\frac{d\vec{\rho}}{dt},\quad \vec{p}_\lambda=m_\lambda\frac{d\vec{\lambda}}{dt}. \quad (2.6)$$

The problem therefore separates into center-of-mass motion plus two independent harmonic oscillators ρ and λ with the same spring constant K but different masses. When all three quarks have the same mass the two oscillators ρ, λ have the same frequency, but not otherwise. The eigenstates of the Hamiltonian (2.4) are well known. The ground state ψ_{00} has both (ρ,λ) oscillators in their respective ground states. The first excited states ψ_{1m}^ρ, ψ_{1m}^λ which concern us here have one or the other of the two oscillators in their first excited state. For example,

$$\psi_{00}(\vec{\rho},\vec{\lambda})=\frac{\alpha_\rho^{3/2}}{\pi^{3/4}}\frac{\alpha_\rho^{3/2}}{\pi^{3/4}}e^{-\alpha_\rho^2\rho^2/2}e^{-\alpha_\lambda^2\lambda^2/2},$$
$$\psi_{11}^\lambda(\vec{\rho},\vec{\lambda})=-\frac{\alpha_\lambda^{5/2}\alpha_\rho^{3/2}}{\pi^{3/2}}(\lambda_x+i\lambda_y)\,e^{-\alpha_\rho^2\rho^2/2}e^{-\alpha_\lambda^2\lambda^2/2}, \quad (2.7)$$

where

$$\alpha_\rho^2=(3Km_\rho)^{1/2}$$
$$\alpha_\lambda^2=(3Km_\lambda)^{1/2}. \quad (2.8)$$

Note from (2.3) that ψ_{1m}^λ is even under the transposition (12), while the analogous wave function ψ_{1m}^ρ is odd.

Usually the difference produced by different quark masses are neglected in spatial wave func-

tions. We will neglect the mass difference between the up and down quarks (on this scale),[12] but do take into account the different mass of the strange quark. As a first approximation, we find that in computing *matrix elements of the perturbation* one may take $\alpha_\rho{}^2 \simeq \alpha_\lambda{}^2$ while remembering that the two oscillators (ρ, λ) are nondegenerate. This is only the case for strange baryons, and will no longer be a good approximation for charmed baryons, which we hope to discuss in a separate paper.

III. ZERO-ORDER WAVE FUNCTIONS

The multiplet of states associated with the negative-parity orbital excitations $\psi^\rho_{1m}, \psi^\lambda_{1m}$ are well known: They are commonly classified in a 70-supermultiplet of SU(6) which breaks into the multiplets ^{2}1, ^{2}8, ^{4}8, and ^{2}10 where the superscripts indicate the total quark spin associated with the SU(3) multiplets. The quark spin S is then added to the orbital angular momentum L to give the total angular momentum J. A list of the states in the SU(6) basis is given in Table I. When there are several states of the same J, strangeness, and isospin the physical states are in general mixed.

In all previous work of which we are aware the wave functions of these physical states are constructed by taking linear superpositions of space, spin, and unitary-spin wave functions which are totally symmetric under the exchange of any two quarks. This is the correct prescription as long as all the quarks have equal mass. This is the case in the $S=0$ and $S=-3$ sectors. When dealing with states containing unequal-mass quarks we only symmetrize between those quarks which have equal mass. This prescription[13] is contingent upon the explicit symmetry breaking in the *orbital* wave functions (2.7).

TABLE I. Low-lying negative-parity baryons in an SU(3) basis.

		^{2}8	^{4}8	^{2}10	^{2}1
$S=0$:	$J=\frac{1}{2}$	N	N	Δ	⋯
	$J=\frac{3}{2}$	N	N	Δ	⋯
	$J=\frac{5}{2}$		N		
$S=-1$:	$J=\frac{1}{2}$	Λ, Σ	Λ, Σ	Σ	Λ
	$J=\frac{3}{2}$	Λ, Σ	Λ, Σ	Σ	Λ
	$J=\frac{5}{2}$	⋯	Λ, Σ	⋯	⋯
$S=-2$:	$J=\frac{1}{2}$	Ξ	Ξ	Ξ	⋯
	$J=\frac{3}{2}$	Ξ	Ξ	Ξ	⋯
	$J=\frac{5}{2}$	⋯	Ξ	⋯	⋯
$S=-3$:	$J=\frac{1}{2}$	⋯	⋯	Ω^-	⋯
	$J=\frac{3}{2}$	⋯	⋯	Ω^-	⋯

We now list with this prescription the space-spin-flavor wave functions of the Λ^0, Σ^0 states, with the convention that the strange quark is particle number 3:

	$^4\rho$ or $^4\lambda$	$^2\rho$	$^2\lambda$
Λ^5_2	$\psi^\rho_{11}\chi^s_{3/2}\phi_0$		
Λ^3_2	$(\,)\psi^\rho_{1m}\chi^s_{3/2-m}\phi_0$	$(\,)\psi^\rho_{1m}\chi^\lambda_{3/2-m}\phi_0$	$(\,)\psi^\lambda_{1m}\chi^\rho_{3/2-m}\phi_0$
Λ^1_2	$(\,)\psi^\rho_{1m}\chi^s_{1/2-m}\phi_0$	$(\,)\psi^\rho_{1m}\chi^\lambda_{1/2-m}\phi_0$	$(\,)\psi^\lambda_{1m}\chi^\rho_{1/2-m}\phi_0$
Σ^5_2	$\psi^\lambda_{11}\chi^s_{3/2}\phi_1$		
Σ^3_2	$(\,)\psi^\lambda_{1m}\chi^s_{3/2-m}\phi_1$	$(\,)\psi^\rho_{1m}\chi^\rho_{3/2-m}\phi_1$	$(\,)\psi^\lambda_{1m}\chi^\lambda_{1/2-m}\phi_1$
Σ^1_2	$(\,)\psi^\lambda_{1m}\chi^s_{1/2-m}\phi_1$	$(\,)\psi^\rho_{1m}\chi^\rho_{1/2-m}\phi_1$	$(\,)\psi^\lambda_{1m}\chi^\lambda_{1/2-m}\phi_1$

(3.1)

where the empty parentheses in front of a wave function indicates summation over the magnetic quantum number m with the appropriate Clebsch-Gordan coefficients, in the LS order, e.g.,

$$|\Lambda^3_2; {}^4\rho\rangle = (\,)\psi^\rho_{1m}\chi^s_{3/2-m}\phi_0$$
$$\equiv \sum_m (1, \tfrac{3}{2}, \tfrac{3}{2}; m\ \ \tfrac{3}{2}-m)\psi^\rho_{1m}\chi^s_{3/2-m}\phi_0$$
$$= (\tfrac{2}{5})^{1/2}\psi^\rho_{11}\chi^s_{1/2}\phi_0 - (\tfrac{3}{5})^{1/2}\psi^\rho_{10}\chi^s_{3/2}\phi_0 .$$

The quartet spin wave functions χ^s_m are the usual ones ($\chi^s_{3/2} = |\uparrow\uparrow\uparrow\rangle$), while the ρ and λ type doublet spin states are

$$\chi^\rho_{1/2} = \frac{1}{\sqrt{2}}(|\downarrow\uparrow\uparrow\rangle - |\uparrow\downarrow\uparrow\rangle),$$
$$\chi^\rho_{-1/2} = \frac{1}{\sqrt{2}}(|\downarrow\uparrow\downarrow\rangle - |\uparrow\downarrow\downarrow\rangle),$$
$$\chi^\lambda_{1/2} = \frac{1}{\sqrt{6}}(|\downarrow\uparrow\uparrow\rangle + |\uparrow\downarrow\uparrow\rangle - 2|\uparrow\uparrow\downarrow\rangle),$$
$$\chi^\lambda_{-1/2} = \frac{1}{\sqrt{6}}(2|\downarrow\downarrow\uparrow\rangle - |\downarrow\uparrow\downarrow\rangle - |\uparrow\downarrow\downarrow\rangle),$$

and the isospin wave functions ϕ_0 and ϕ_1 are

$$\phi_0 = \frac{1}{\sqrt{2}}(ud - du)s ,$$
$$\phi_1 = \frac{1}{\sqrt{2}}(ud + du)s .$$

It is worth noting that the wave functions (3.1) are simpler than the usual choice of completely symmetrized states.

While the quartet spin states have ^{4}8 states as their limit when $m_s = m_d$, the states $|\Lambda; {}^2\rho\rangle$, $|\Lambda; {}^2\lambda\rangle$, $|\Sigma, {}^2\rho\rangle$, and $|\Sigma, {}^2\lambda\rangle$ do not have individual SU(3) states as their limit, but

$$|\Lambda;^2 1> = \lim_{m_s \to m_d} \frac{1}{\sqrt{2}}(|\Lambda;^2\lambda> - |\Lambda;^2\rho>),$$

$$|\Lambda;^2 8> = \lim_{m_s \to m_d} \frac{1}{\sqrt{2}}(|\Lambda;^2\rho> + |\Lambda;^2\lambda>),$$

$$|\Sigma;^2 8> = \lim_{m_s \to m_d} \frac{1}{\sqrt{2}}(|\Sigma;^2\rho> - |\Sigma;^2\lambda>),$$

$$|\Sigma;^2 10> = \lim_{m_s \to m_d} \frac{1}{\sqrt{2}}(|\Sigma;^2\rho> + |\Sigma;^2\lambda>).$$

(These equations should be understood only in the sense of matrix elements of both sides being equal.) The actual physical states are neither pure SU(3) states nor pure ρ (or λ) excitations but linear combinations of all substates with the same J, strangeness, and isospin. Most physical states are, however, closer to pure ρ or λ states than to pure SU(3) eigenstates. The linear combinations quoted in the literature are[10] in terms of an SU(3) basis, which is why we need these transformations.

The N, Δ, Ξ, Ω^- states can be constructed in a similar way. However, it is unnecessary to construct their wave functions since the relevant matrix elements may be inferred from those of the Λ^0, Σ^0 sector by either taking (i) $m = m' = m_d$ (N's, Δ's), (ii) $m = m' = m_s$ (Ω^-'s), or $m = m_s$ and $m' = m_d$ (Ξ's).

IV. COMPARISON WITH EXPERIMENT

We relegate an account of some of the details of the calculation of the hyperfine matrix elements to Appendix A, but mention a few points here before quoting the results. While these computations are simple in principle they tend to be long, and so the authors have taken the precaution of calculating separately each matrix element until agreement is reached. The matrix elements of the contact term are relatively simple to calculate. As mentioned earlier, the contact term operates only between quarks that are in relative S waves, so that, for example, there is no contribution of H^{12}_{contact} in a ψ^{ρ}_{1m}. Even when one keeps $\alpha_\rho \neq \alpha_\lambda$ one can still invoke symmetry properties in these calculations: It is still true that the matrix elements of H^{13}_{contact} and H^{23}_{contact} are equal. An additional simplicity arises from the fact that there are no matrix elements of H_{contact} connecting quark spin-$\frac{1}{2}$ states to quark spin-$\frac{3}{2}$ states, since H_{contact} is a spin-zero operator.

The matrix elements of the tensor term are more trouble to evaluate; fortunately, many of the matrix elements are zero. This is because H_{tensor} is a spin-2 operator and so cannot connect quark spin $\frac{1}{2}$ to quark spin $\frac{1}{2}$. One can also make use of the fact that H^{12}_{tensor} vanishes in ψ^{λ}_{1m} states since such states have quarks 1 and 2 in a relative S wave; furthermore, matrix elements of H^{13}_{tensor} and H^{23}_{tensor} are equal, as the reasons applied in the case of the contact term continue to hold.

The relevant matrix elements of the hyperfine interaction are computed and displayed in Appendix A. One must add this interaction to the unperturbed Hamiltonian. In the $S = -1$ sector, for example, this amounts to remembering that the ρ oscillator is not degenerate with the λ oscillator. In the harmonic-oscillator model the frequency of the ρ oscillator is higher than that of the λ oscillator by

$$\omega_\rho - \omega_\lambda = \omega\left[1 - \left(\frac{2x+1}{3}\right)^{1/2}\right], \tag{4.1}$$

where $x = m_d/m_s$ and $\hbar\omega = \hbar\omega_\rho$ is the harmonic-oscillator spacing in the $S = 0$ sector. The harmonic-oscillator model also predicts the relative position of all ($S = 0$, $S = -1$, $S = -2$, $S = -3$) sectors given $\hbar\omega$, m_d, and m_s. This is discussed in Appendix B. Without harmonic oscillators these quantities are undetermined parameters; nevertheless we believe the harmonic-oscillator values to be typical also for other potentials.

We are now ready to diagonalize the resulting matrices sector by sector and compare to experiment. The results for all sectors are displayed in Table II and in Figs. 1, 2, 3, and 4.

A. The $S = 0$ sector of N^*'s and Δ^*'s

There is little to add to the discussion in I of these states. The agreement with the observed masses is good. The size of the splitting here has been related to the Δ-N splitting in the ground state. The tensor force gives strong mixing in the $N^*\frac{1}{2}^-$ sector, but very little mixing in the $N^*\frac{3}{2}^-$ sector as observed. This, to our knowledge, was not previously understood. The predicted mixing angles are in very good agreement with the magnitude *and* sign obtained by the decay analyses. We stress that our conclusions about mixing angles are independent of any parameters.

B. The $S = -1$ sector of Λ's and Σ's

The experimental data shown in the figures for this sector are based on the four multichannel $\bar{K}N$ phase-shift analyses known to us[14] [except for $\Lambda^*\frac{1}{2}^-(1405)$ which is below threshold]. We show those resonances which have been seen in at least two of the four analyses, and choose the shaded region to encompass the quoted mass values. (There are additional candidates seen only in one analysis.) This mass region agrees with the likely mass region suggested by the Particle Data Group in all cases except for the $\Sigma^*\frac{1}{2}^-(1770)$ and $\Sigma^*\frac{3}{2}^-(1940)$ (where the disagreement is relatively mild).

The mass difference between the $J = \frac{5}{2}^-$ Σ and Λ is primarily a spin-independent effect due to the lack

TABLE II. Predicted masses and compositions of negative-parity baryons.

State	Predicted splitting [a] from unperturbed mass in units of δ	Predicted mass (MeV)		Predicted (**) and measured composition [b] ^{2}1	^{2}8	^{4}8	^{2}10
$N^*\frac{1}{2}^-$	−0.40	1490	**	•••	+0.85	+0.53	•••
			HLC	•••	+0.85	+0.53	•••
			FP	•••	+0.73	+0.68	•••
$N^*\frac{1}{2}^-$	+0.15	1655	**	•••	+0.53	−0.85	•••
			HLC	•••	+0.53	−0.85	•••
			FP	•••	+0.68	−0.73	•••
$\Delta^*\frac{1}{2}^-$	+0.25	1685	**				
$\Lambda^*\frac{1}{2}^-$	−0.69 [c]	1490	**	+0.90	+0.43	+0.06	•••
			HLC	+0.85	+0.46	+0.25	•••
			FP1	+0.79	+0.61	−0.04	•••
			FP2	+0.72	+0.68	+0.14	•••
$\Lambda^*\frac{1}{2}^-$	−0.16	1650	**	−0.39	+0.75	+0.58	•••
			HLC	−0.30	+0.04	+0.95	•••
			FP1	−0.44	+0.63	+0.64	•••
			FP2	−0.32	+0.15	+0.94	•••
$\Lambda^*\frac{1}{2}^-$	+0.34	1800	**	−0.18	+0.50	−0.85	•••
			HLC	−0.43	+0.89	−0.17	•••
			FP1	−0.41	+0.49	−0.77	•••
			FP2	−0.62	+0.71	−0.32	•••
$\Sigma^*\frac{1}{2}^-$	−0.17	1650	**	•••	+0.82	+0.54	−0.17
$\Sigma^*\frac{1}{2}^-$ [d]	+0.17	1750	**	•••	−0.46	+0.81	+0.35
$\Sigma^*\frac{1}{2}^-$ [d]	+0.36	1810	**	•••	+0.33	−0.21	+0.92
$\Xi^*\frac{1}{2}^-$	−0.41	1780	**	•••	+0.88	+0.42	+0.22
$\Xi^*\frac{1}{2}^-$	−0.01	1900	**	•••	−0.18	+0.73	−0.66
$\Xi^*\frac{1}{2}^-$	+0.11	1930	**	•••	+0.43	−0.56	−0.73
$\Omega^*\frac{1}{2}^-$	+0.13	2020	**				
$N^*\frac{3}{2}^-$	−0.26	1535	**	•••	0.99	−0.11	•••
			HLC	•••	0.98	−0.18	•••
			FP	•••	0.97	−0.26	•••
$N^*\frac{3}{2}^-$	+0.46	1745	**	•••	0.11	+0.99	•••
			HLC	•••	0.18	0.98	•••
			FP	•••	0.26	0.97	•••
$\Delta^*\frac{3}{2}^-$	+0.25	1685	**				
$\Lambda^*\frac{3}{2}^-$	−0.69 [c]	1490	**	+0.91	+0.40	−0.01	•••
			HLC	+0.92	+0.39	−0.04	•••
$\Lambda^*\frac{3}{2}^-$	−0.03	1690	**	−0.40	+0.91	−0.12	•••
			HLC	−0.39	+0.92	+0.00	•••
$\Lambda^*\frac{3}{2}^-$	+0.61	1880	**	−0.04	+0.11	+0.99	•••
			HLC	−0.04	+0.01	+1.00	•••

TABLE II. *(continued)*

State	Predicted splitting [a] from unperturbed mass in units of δ	Predicted mass (MeV)		Predicted (**) and measured composition [b] ^{2}1	^{2}8	^{4}8	^{2}10
$\Sigma^*\frac{3}{2}^-$	−0.08	1675	**	···	+0.96	−0.11	−0.26
			HLC	···	+0.89	−0.38	+0.26
			FP	···	+0.88	+0.07	−0.46
$\Sigma^*\frac{3}{2}^-$	+0.35	1805	**				
$\Sigma^*\frac{3}{2}^-$	+0.38	1815	**	···	+0.25	+0.76	+0.60
$\Xi^*\frac{3}{2}^-$	−0.34	1800	**	···	+0.96	−0.08	−0.30
$\Xi^*\frac{3}{2}^-$	+0.07	1920	**	···	+0.29	−0.09	+0.95
$\Xi^*\frac{3}{2}^-$	+0.29	1985	**	···	+0.10	+0.99	+0.06
$\Omega^*\frac{3}{2}^-$	+0.13	2020	**				
$N^*\frac{5}{2}^-$	+0.20	1670	**				
$\Lambda^*\frac{5}{2}^-$	+0.38	1815	**				
$\Sigma^*\frac{5}{2}^-$	+0.20	1760	**				
$\Xi^*\frac{5}{2}^-$	+0.10	1930	**				

[a] These are the eigenvalues relative to the unperturbed position of a λ-type oscillator in the relavant space of states, using either $x=0.7$ and approximate formulas ($\alpha_\rho=\alpha_\lambda$) of Tables III and IV or $x=0.6$ and the exact formulas $\alpha_\rho \neq \alpha_\lambda$ for the $S=-1$ sector.

[b] The FP results quoted here have been converted to HLC phase conventions.

[c] These results both include an additional −0.12 units of splitting arising from second-order effects. No other state any had significant second-order effects [in the SU(3) limit ^{2}1 is perturbed three times as much as any other state].

[d] Since the observed Σ(1750) is actually midway between these two predictions, it makes no sense to quote an experimental composition until the situation in this region is resolved.

of degeneracy between the ρ and λ oscillator. Both of these states have quark spin $S=\frac{3}{2}$; this spin state is symmetric under interchange of any two quarks. The flavor wave function of the Σ ($I=1$) is also even under interchange of u and d quarks. Therefore, Σ corresponds to the even oscillator (λ) being excited. The flavor state of the Λ($I=0$) is odd under interchange of u and d quarks. Therefore, the Λ corresponds to the odd oscillator (ρ) being excited. Because the strange quark is heavier than the nonstrange quarks, the two oscillators are nondegenerate. The λ oscillator in which the heavier quark moves has the lower frequency, and correspondingly the $\Sigma^*\frac{5}{2}^-$ is lighter than the $\Lambda^*\frac{5}{2}^-$. In the harmonic-oscillator model this mass difference [see (4.1)] is about 75 MeV $\equiv(\hbar\omega_\rho-\hbar\omega_\lambda)$ and hyperfine interactions give a relatively small correction (~20 MeV) to this effect.

The $\Lambda^*\frac{3}{2}^-$ sector is also very well reproduced, with good agreement for the masses and compositions of $\Lambda^*\frac{3}{2}^-(1520)$ and $\Lambda^*\frac{3}{2}^-(1690)$. The third $\Lambda^*\frac{3}{2}^-$ state is predicted to lie very high at around 1880 MeV and to be an almost pure ^{4}8 state (and therefore decoupled from $\bar{K}N$, which may account for its not having been seen). The information in the $\Sigma^*\frac{3}{2}^-$ sector is quite sketchy. We correctly obtain the mass of the well established $\Sigma^*\frac{3}{2}^-(1675)$ and correctly predict that it is dominantly a ^{2}8 state. The two decay analyses[10] do not agree on the admixtures of ^{4}8 and ^{2}10 into this state, and we do not agree with either of them. We predict that the other two $\Sigma^*\frac{3}{2}^-$ states will be nearly degenerate at ~1810 MeV; this prediction is very specific to harmonic-oscillator forces. In any case, this degeneracy will almost certainly be broken by mixing via decay channels.

The $\Lambda^*\frac{1}{2}^-(1405)$ is, of the well-established states, the one farthest from its expected mass. Its composition is, however, in quite good agreement with experiment,[10] especially with HLC and solution 1 of FP. We do not understand this discrepancy, although several possibilities suggest themselves: (1) The $\Lambda^*\frac{1}{2}^-(1405)$ has been shifted from its bound-state position by its proximity to $\bar{K}N$ threshold. It is well known that mass shifts due to mixing with virtual decay channels can be quite strong near a threshold; such an effect could depress this state significantly since it is strongly coupled to $\bar{K}N$.

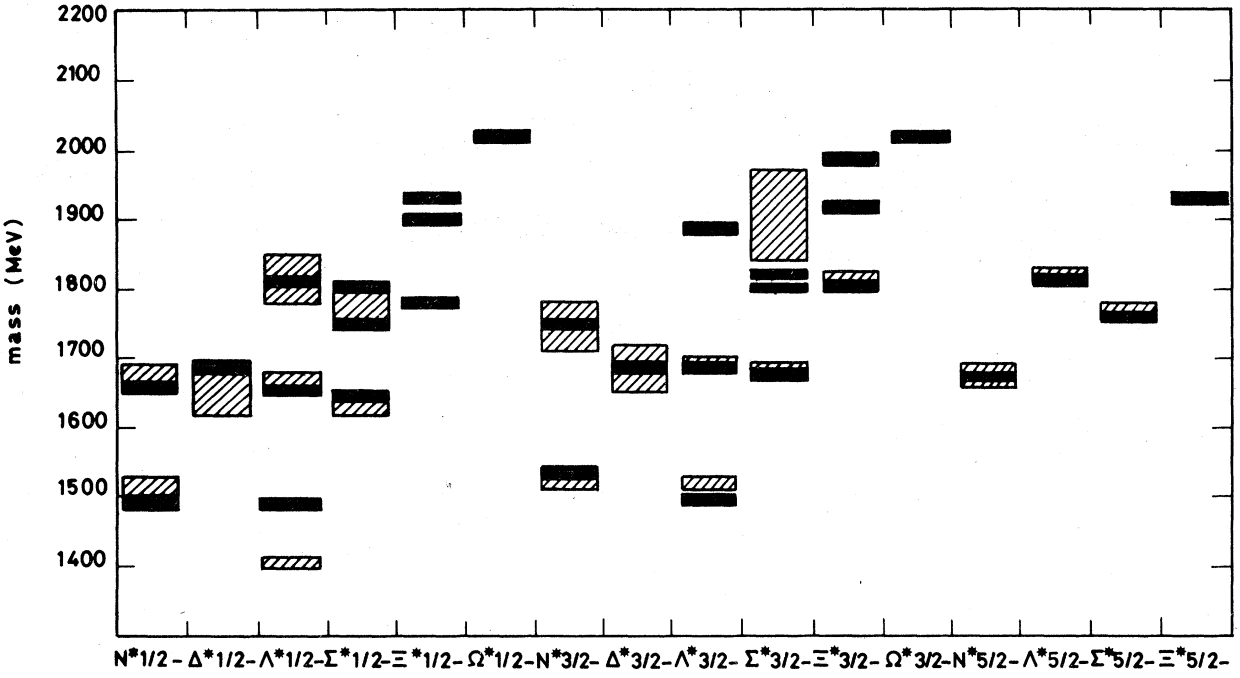

FIG. 1. Comparison of the predicted and observed spectrum of negative-parity baryons. The shaded regions correspond to the likely mass values of resonances; the solid bars are the predictions of the text, corresponding to the parameters $m_0 = 1610$ MeV, $\omega = 520$ MeV, $x = 0.6$, $\Delta m = 280$ MeV, and $\delta = 300$ MeV.

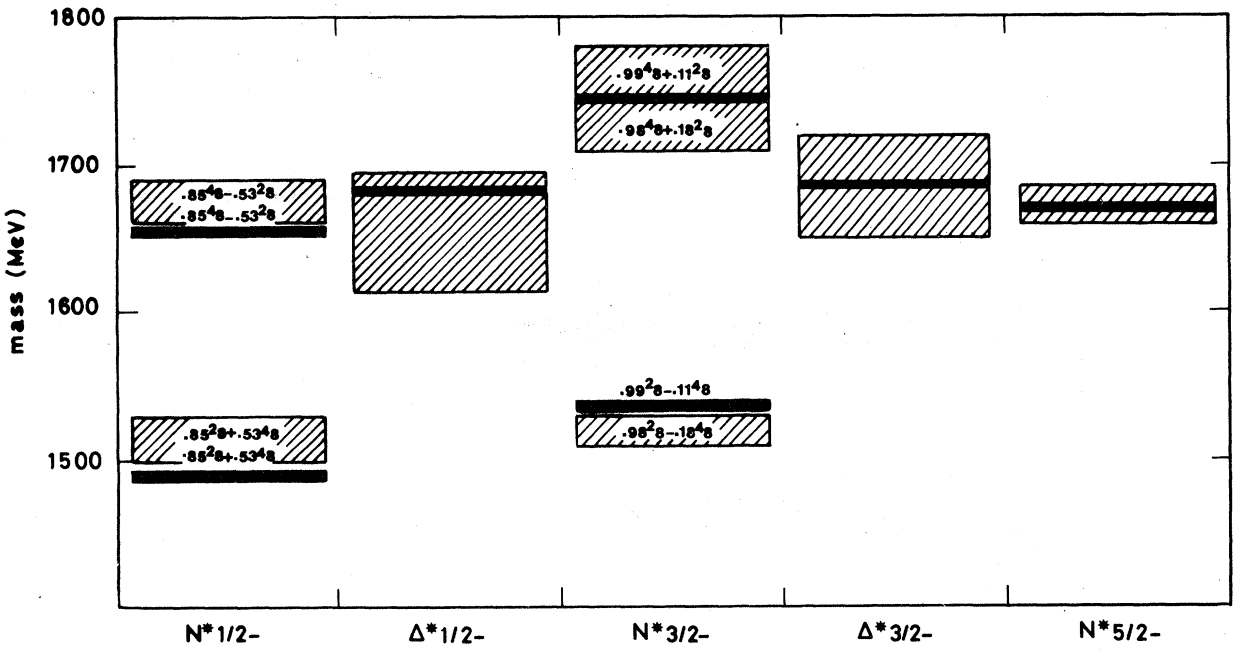

FIG. 2. Comparison of the predicted and observed spectrum of negative-parity $S = 0$ baryons. The predicted composition of a given state is displayed directly above the bar indicating its position. The experimental composition is given in the most convenient location with respect to the shaded region which indicates its experimental position.

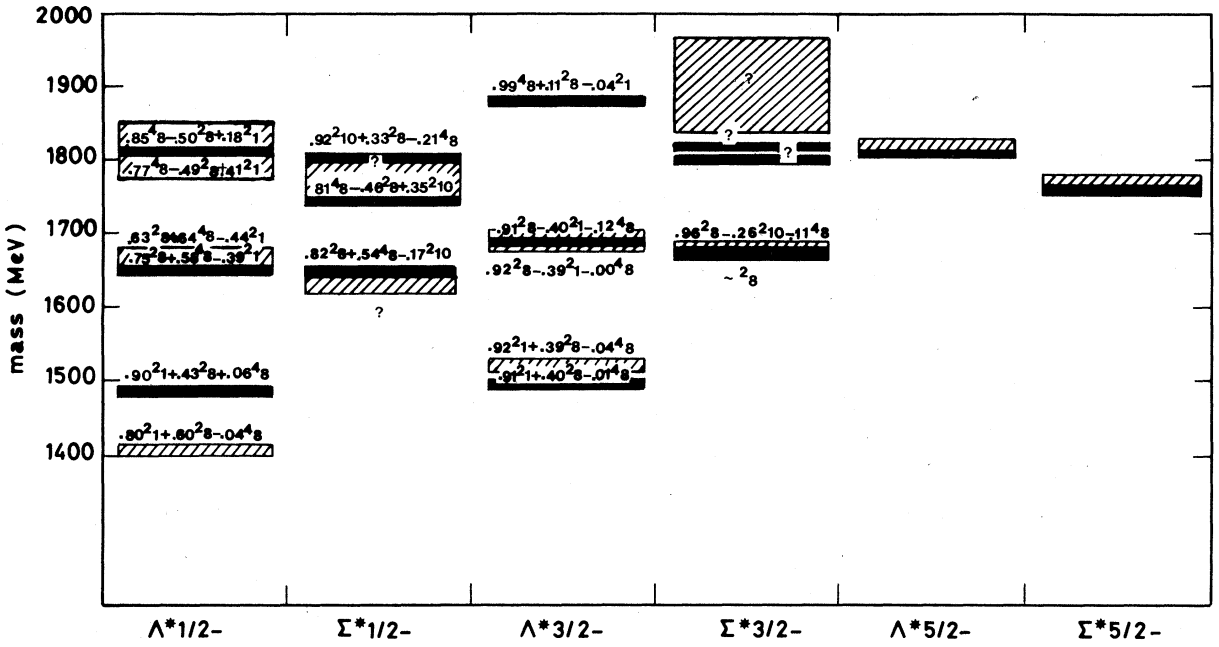

FIG. 3. Comparison of the predicted and observed spectrum of negative-parity $S=-1$ baryons.

(2) The residual spin-orbit couplings, which we have neglected throughout, have resurfaced in this state (this possibility gets some support from the discussion of Sec. V. (3) The predicted near degeneracy of the lowest $\Lambda^*\frac{1}{2}^-$ and $\Lambda^*\frac{3}{2}^-$ states is specific to the harmonic oscillator (see Sec. VI). The masses of the remaining two $\Lambda^*\frac{1}{2}^-$ states are rather neatly predicted, but the situation regarding their composition is unclear. The decay analyses here find two quite different solutions: a solution A which corresponds to the HLC solution and to solution 2 of FP, and a solution B which corresponds to solution 1 of FP. We would argue that solution A should be viewed with some skepticism as it has the dominantly ^{4}8 and ^{2}8 states reversed relative to the $N^*\frac{1}{2}^-$ sector.[10] In any event, our

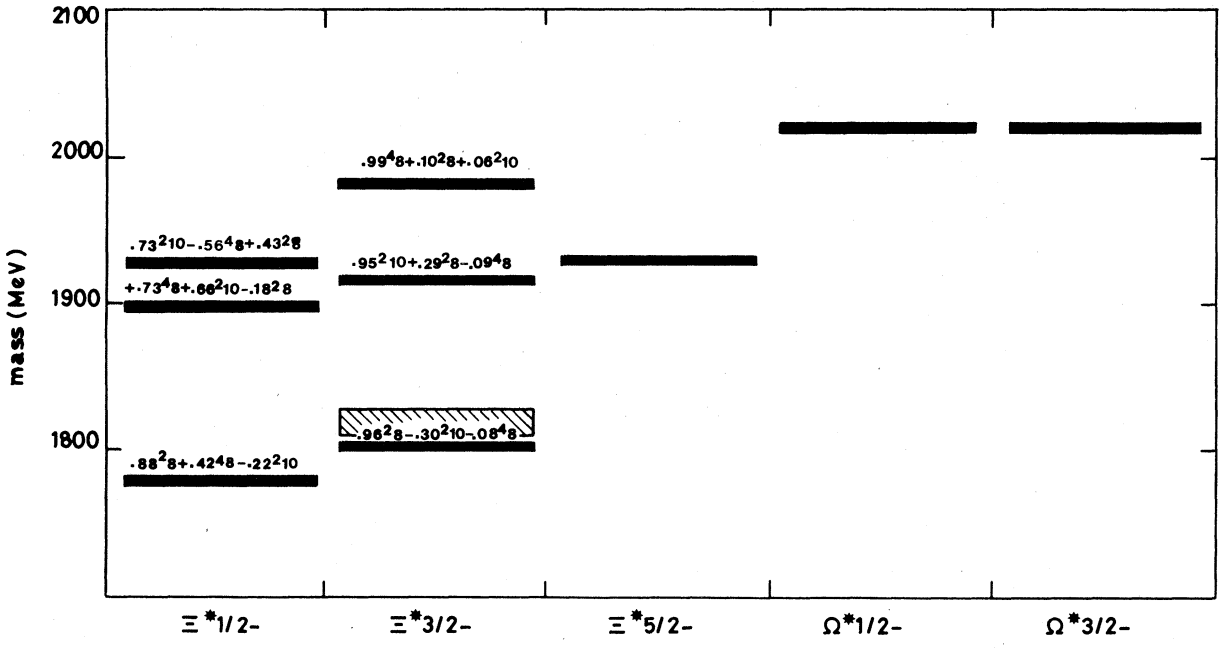

FIG. 4. Comparison of the predicted and observed spectrum of negative-parity $S=-2$ and $S=-3$ baryons.

predictions are in good agreement with the SU(3)-like solution B (i.e., solution 1 of FP). This solution can be clearly differentiated from solution A experimentally by a measurement of the sign of the amplitude for $N\bar{K} \to \Lambda(1670) \to \Lambda\eta$. Such a measurement would consititute an important test of our model.

Finally, in the $\Sigma^*\frac{1}{2}^-$ sector we correctly obtain the mass of the $\Sigma^*\frac{1}{2}^-(1620)$ and bracket with our remaining two predictions the effect seen in the S11 partial wave from 1750–1800 MeV. There is no information on the composition of $\Sigma^*\frac{1}{2}^-(1620)$ and until the situation in the region from 1750 to 1800 MeV is resolved, any conclusions about the compositions of states would be dangerous.

C. The $S = -2$ and -3 sectors of Ξ^*'s and Ω^*'s

Our results on these two sectors are almost entirely predictive. The only exception is the $\Xi^*(1820)$ which is probably $\frac{3}{2}^-$.

We should remind the reader at this point that the most reliable features of these predictions are the splittings and mixing angles; the positions of the unperturbed $Y = -1$ and -2 masses are a separate issue, as disucssed in Appendix B.

V. WHERE HAS ALL THE SPIN-ORBIT COUPLING GONE?

The success of the simple Hamiltonian (2.1) in describing the complex pattern of P-wave baryons immediately raises several questions. If we are to think of these results as establishing the existence of an interaction between two color magnetic moments, then we must try to understand why these states show no evidence for the existence of spin-orbit forces which could arise, in part, from an interaction of the color magnets with the magnetic fields due to the orbital motion. We have from the beginning neglected spin-orbit forces. It is certainly relevant to ask what the effect of spin-orbit forces would be, or put another way, to ask what strength of spin-orbit forces are indicated by the data. Our conclusion is that spin-orbit forces, if present at all, are at a level much reduced over naive expectations.

To make this statement more precise, we introduce the spin-orbit forces which arise from one-gluon exchange in chromodynamics,

$$H_{SO(1G)} = \sum_{i<j} H^{ij}_{SO(1G)}, \tag{5.1}$$

where

$$H^{ij}_{SO(1G)} = \frac{\alpha_s}{3r_{ij}^3}\left(\frac{\vec{S}_i\cdot\vec{r}_{ij}\times\vec{p}_i}{m_i^2} - \frac{\vec{S}_j\cdot\vec{r}_{ij}\times\vec{p}_j}{m_j^2} - \frac{2\vec{S}_i\cdot\vec{r}_{ij}\times\vec{p}_j - 2\vec{S}_j\cdot\vec{r}_{ij}\times\vec{p}_i}{m_i m_j}\right). \tag{5.2}$$

It is surprising that this force seems to have three-body components.[9] For example,

$$H^{12}_{SO(1G)} = \frac{\alpha_s}{m^2 r_{12}^3}\left[(\vec{S}_1+\vec{S}_2)\cdot(\vec{\rho}\times\vec{p}_\rho) - \frac{1}{3\sqrt{3}}(\vec{S}_1-\vec{S}_2)\cdot(\vec{\rho}\times\vec{p}_\lambda)\right], \tag{5.3}$$

where m, $\vec{\rho}$, $\vec{p}_\rho$, and $\vec{p}_\lambda$ are defined in Sec. II. We have calculated all the 70 1^- matrix elements of $H_{SO(1G)}$ using the same techniques as employed in the calculations with H_{hyp}. The complete results are displayed in Appendix C; a good feeling for the situation can, however, be obtained simply by examining the effect of $H_{SO(1G)}$ on the N^* sector alone. It is not hard to see by looking at the trace of $H_{SO(1G)}$ in the $N^*\frac{1}{2}^-$ states that the center of gravity of the two $N^*\frac{1}{2}^-$ states will be lowered by $\frac{13}{8}\delta$ with respect to its position in Figs. 1 and 2 relative to the $N^*\frac{5}{2}^-$. But this amounts to almost 500 MeV and so is totally out of the question. On this basis we could argue that in the absence of other effects $H_{SO(1G)}$ must be present at no more than about 10% of its full strength. A more detailed analysis based on the full results of Appendix C confirms this conclusion, which is very similar to conclusions which have been drawn concerning the spin-orbit forces in charmonium.[4,5]

While we have no convincing explanation for this observation, we would like to make a few speculative comments. First of all, one could imagine that the quark-gluon color magnetic moment is highly anomalous.[4] This would automatically make spin-spin interactions dominant over spin-orbit ones. Although we do not find this explanation very appealing it is a possibility.

An alternative explanation is that the matrix elements of $H_{SO(1G)}$ are as calculated, but that they are canceled by some other effect. If such a cancellation were to occur in each state, the effect in question would have to be of a spin-orbit type. There is in fact a spin-orbit coupling which we have, up to this point, failed to consider: Although the long-range confining force is presumably spin independent,[1a] *it will still contribute to the spin-orbit interaction through Thomas precession.* It is, moreover, quite clear that this tends to cancel with $H_{SO(1G)}$. As is well known, the sign of the Thomas precession term in a $1/r$ potential is opposite to the sign of the part of the spin-orbit precession arising from the interaction of the magnetic moment with the magnetic fields due to the orbital motion. This sign is determined only by the fact that the potential is attractive, and leads to a reduction of the spin-orbit interaction strength by the famous factor of 2. Now consider a quark which is far away from the other quarks. It will

feel a negligible spin-orbit force from $H_{SO(1G)}$ but will feel a strong spin-orbit interaction from the confining potential that is once again of opposite sign to $H_{SO(1G)}$. It follows that at some interquark distance the spin-orbit interaction must change sign, at which point it of course vanishes. The crucial feature is the relation of this point to the typical interquark distance in these states. We have accordingly considered the spin-orbit interaction due to a harmonic potential,

$$H_{\text{Thom(HO)}} = \sum_{i<j} H^{ij}_{\text{Thom(HO)}}, \tag{5.4}$$

where

$$H^{ij}_{\text{Thom(HO)}} = -\tfrac{1}{2}K\left[\frac{\vec{S}_i\cdot\vec{r}_{ij}\times\vec{p}_i}{m_i^2} - \frac{\vec{S}_i\cdot\vec{r}_{ij}\times\vec{p}_j}{m_j^2}\right]. \tag{5.5}$$

This interaction, like $H_{SO(1G)}$, also has both two- and three-body components. For example,

$$H^{12}_{\text{Thom(HO)}} = -\frac{K}{2m^2}\left[(\vec{S}_1+\vec{S}_2)\cdot(\vec{\rho}\times\vec{p}_\rho) + \frac{1}{\sqrt{3}}(\vec{S}_1-\vec{S}_2)\cdot(\vec{\rho}\times\vec{p}_\lambda)\right]. \tag{5.6}$$

The matrix elements of $H_{\text{Thom(HO)}}$ are given in Appendix C. With $\omega \simeq 500$ MeV and $m \simeq 350$ MeV *there is an almost perfect cancellation between the two-body parts* of $H_{SO(1G)}$ and $H_{\text{Thom(HO)}}$ in the SU(3) limit. A further enticing feature of this cancellation is that in breaking SU(3) the only significant change that occurs in the spectrum is that the lowest $\Lambda^*\frac{1}{2}^-$ is lowered by ~40 MeV and the lowest $\Lambda^*\frac{3}{2}^-$ is raised by ~20 MeV, thereby significantly improving agreement with experiment.

Though this result is intriguing, it cannot be the whole story since such a cancellation does not also occur in the three-body spin-orbit terms. Even though the three-body terms are generally smaller than the two-body terms, without some cancellation they still perturb our results in an intolerable way. One way out of this problem would be to argue that since the confining force must necessarily have three-body components which the harmonic-oscillator model does not take into account, the three-body terms in the spin-orbit interaction cannot be reliably calculated. This may be so, but it is a suggestion which we do not know yet how to check. Another possibility is that the three-body terms are not actually present; their derivation is not straightforward and it is conceivable that they are simply spurious.[16] In any event, a weakness of this line of thought is that the cancellation which occurs in the two-body terms is quite model dependent (recall, for example, Ref. 16).

In conclusion: Spin-orbit coupling is certainly small in these states, though the actual reasons remain somewhat obscure.

VI. BEYOND HARMONIC OSCILLATORS

The above analysis can easily be generalized to *arbitrary* orbital wave functions ψ^ρ_{1m}, ψ^λ_{1m}. This is simply done by considering the relevant matrix elements of the type $\langle\psi^\lambda_{11}|\delta^3(\vec{\rho})|\psi^\lambda_{11}\rangle$ and $\langle\psi^\rho_{11}|\rho^{-3}P_2(\cos\theta_\rho)|\psi^\rho_{11}\rangle$ as arbitrary parameters at our disposal. We then lose the ability to relate these two matrix elements to each other and to other quantities such as the expectation value $\langle\psi_{00}|\delta^3(\vec{\rho})|\psi_{00}\rangle$ (relevant to the Δ-N mass difference). Therefore we have two independent parameters which characterize the strength of hyperfine interactions and the relative amplitude y of the tensor term to that of the contact term in a given sector of the negative-parity baryons. Although we lose some predictive power, we have so many states available that we can still test the predictions of the interaction (2.1) this time without making any specific assumptions about the orbital wave functions of the quarks.

While we have not performed an exhaustive fit of this type, we did check the Λ and Σ $\frac{1}{2}^-$ and $\frac{3}{2}^-$ states in the approximation in which the distortion of the wave functions ψ^ρ, ψ^λ (due to $m_s \neq m_u$) is neglected. In this approximation we find that the data would choose a ratio y of the tensor matrix element relative to the contact matrix element rather near the value $y = 1$ appropriate to harmonic-oscillator wave functions. This is illustrated in Fig. 5, which displays the masses of the $\Lambda\frac{1}{2}^-$ and $\Lambda\frac{3}{2}^-$ states as a function of y.

It is seen that the mass of the two lowest-lying $\Lambda\frac{3}{2}^-$ states are not very sensitive to the value of y. Although these two states $\Lambda(1520)$ and $\Lambda(1690)$ are well predicted in the harmonic-oscillator analysis, we learn that these two masses do not in fact test the ratio y. On the other hand, the mass of the lowest-lying $\Lambda\frac{1}{2}^-$ state is a very sensitive function of the ratio y, and as the strength of the tensor term increases the mass decreases. Since experimentally the $\Lambda(1405)$ is well below the $\Lambda\frac{3}{2}^-(1520)$ an increase in y can provide a mechanism for the splitting of these two states. It is unlikely, however, that the observed splitting of the $\Lambda(1405)$ is entirely due to this mechanism, since there are two difficulties when y is larger than about 1.5–2. First, one notes that the first excited $\Lambda\frac{1}{2}^-$ state also decreases rapidly in mass as y increases; however, the harmonic-oscillator ($y = 1$) prediction for this state (~1650 MeV) is in good agreement with the experimental value (1660 MeV), whereas for $y = 1.5$ this state would lie at 1610 MeV which is rather poor. Second, as the value of y increases the spin quartet component in the lowest-lying $\frac{1}{2}^-$ state increases rapidly; even by $y = 2$ this amplitude is predicted to be 0.37, whereas the largest

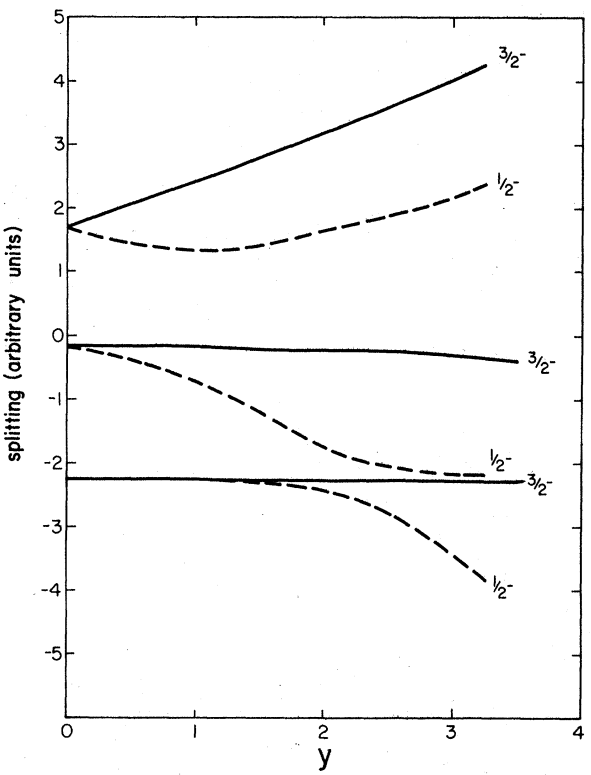

FIG. 5. The masses of the $\Lambda(\frac{3}{2}^-)$ and $\Lambda(\frac{1}{2}^-)$ baryons as a function of the variable y defined in the text of Sec. VI. The value $y=0$ corresponds to no tensor forces while $y=1$ is appropriate to harmonic-oscillator wave functions.

value reported for this quantity is 0.25 (in the analysis of Hey, Litchfield, and Cashmore). Therefore the largest value of y compatible with this piece of information is about $y=1.7$.

In summary, by looking at the four lowest-lying states $\Lambda\frac{1}{2}^-$, $\frac{3}{2}^-$ the best fit to their masses *and* compositions is rather near $y=1$, the harmonic-oscillator value. We stress that the best indications we have for the ratio y come from mixing angles and not from the masses of the states.

VII. SUMMARY, CONCLUSIONS, AND OUTLOOK

Our concern here has been restricted to the most immediate issues raised by the application of QCD-inspired interactions to negative-parity baryons. It is quite clear that the data agree with the hyperfine interactions between quarks proposed by De Rújula *et al.*, but without spin-orbit coupling. We find it difficult not to be impressed by the overall goodness of the "predictions" which are based on the simple Hamiltonian (2.1) with parameters chosen from the ground-state baryons. What is especially pleasing is that the tensor term which plays no role in the ground-state $L=0$ multiplet has the correct strength as predicted from (2.1) with harmonic-oscillator wave functions. We believe this particular conclusion to be quite new.

One other feature of the present analysis again deserves separate mention: The splitting between the $J=\frac{5}{2}$ Λ and Σ states provides good support for the popular idea of a confining potential which is independent of quark mass. This splitting illustrates the removal of degeneracy between the two normal modes of the three-quark system brought about by the heavier mass of the strange quark.

There is a whole ensemble of more advanced questions which are raised by this analysis. We already discussed the mystery of no spin-orbit coupling in Sec. V. Another question, which we have not discussed, concerns the precise[18] value of α_s required by this analysis and whether it is consistent with the coupling of light quarks to gluons as known from other places. These and other related questions deserve separate and careful analysis, which is, however, outside the framework of the present paper.

The most immediate extensions of the calculations reported here are to negative-parity baryons containing a charmed quark and to positive-parity $L=2^+$ states of the three-quark system. We hope to report subsequently on these states. The most important issue still remains that of how to connect this and other phenomenological analyses with the more fundamental theory of chromodynamics. We hope this gap will eventually be bridged.

Note added in proof. The breaking of the degeneracy between the ρ and λ states discussed here provides a dynamical justification for an empirical mixing scheme previously proposed by W. P. Petersen and J. L. Rosner [Phys. Rev. D 6, 820 (1972)] and by D. Faiman [Phys. Rev. D 15, 854 (1977)]. We discuss this in more detail in Phys. Lett. 74B, 353 (1978), where we also note the correspondence of our work with a bag-model discussion of T. A. De Grand and R. L. Jaffee [Ann. Phys. (N.Y.) 100, 425 (1976)].

ACKNOWLEDGMENT

This research was supported in part by the National Research Council of Canada and by the Connaught Fund of the University of Toronto.

APPENDIX A: COMPUTATION OF MATRIX ELEMENTS OF THE HYPERFINE INTERACTION

1. Contact terms

As an example we show the computation of matrix elements of the three contact terms $H^{12}_{\rm cont}$, $H^{13}_{\rm cont}$, and $H^{23}_{\rm cont}$ in the state $\psi^\rho_{11}\chi^S_{3/2}\phi_0$ appropriate to $\Lambda^0\frac{5}{2}^-$. The simplest case corresponds to the contact interaction between quarks 1 and 2:

$$\langle\psi^\rho_{11}\chi^S_{3/2}|H^{12}_{\rm cont}|\psi^\rho_{11}\chi^S_{3/2}\rangle=\frac{2\alpha_s}{3m_d{}^2}\frac{8\pi}{3}\langle\psi^\rho_{11}|\delta^3(\vec{\mathbf{r}}_{12})|\psi^\rho_{11}\rangle \times\langle\chi^S_{3/2}|\vec{\mathbf{S}}_1\cdot\vec{\mathbf{S}}_2|\chi^S_{3/2}\rangle, \quad \text{(A1)}$$

where we dropped the isospin wave function which is not involved. This matrix element vanishes because ψ^ρ_{1m} has to vanish when $\vec{r}_{12}=0$ since it is antisymmetric under the exchange (12).

We turn now to the contact interaction between quarks 1 and 3 (recall that quark 3 is strange), which can be related to an interaction between quarks 1 and 2 by using permutations:

$$\langle\psi^\rho_{11}\chi^S_{3/2}|H^{13}_{\rm cont}|\psi^\rho_{11}\chi^S_{3/2}\rangle = \langle\psi^\rho_{11}\chi^S_{3/2}|(23)(23)H^{13}_{\rm cont}(23)(23)|\psi^\lambda_{11}\chi^S_{3/2}\rangle, \quad \text{(A2)}$$

where

$$(23)H^{13}_{\rm cont}(23)=\frac{m_d}{m_s}H^{12}_{\rm cont}=xH^{12}_{\rm cont},$$
$$(23)\chi^S_{3/2}=\chi^S_{3/2}, \quad \text{(A3)}$$
$$(23)\psi^\rho_{11}=\tfrac{1}{2}\psi^\rho_{11}+\frac{\sqrt{3}}{2}\psi^\lambda_{11},$$

and therefore

$$\langle\psi^\rho_{11}\chi^S_{3/2}|H^{13}_{\rm cont}|\psi^\rho_{11}\chi^S_{3/2}\rangle=\tfrac{3}{4}x\langle\psi^\lambda_{11}\chi^S_{3/2}|H^{12}_{\rm cont}|\psi^\lambda_{11}\chi^S_{3/2}\rangle \quad \text{(A4)}$$
$$=\frac{3x}{4}\frac{16\pi\alpha_s}{9m_d^2}\langle\psi^\lambda_{11}|\delta^3(\vec{r}_{12})|\psi^\lambda_{11}\rangle \times\langle\chi^S_{3/2}|\vec{S}_1\cdot\vec{S}_2|\chi^S_{3/2}\rangle$$
$$=\frac{x\pi\alpha_s}{3m_d^2}\langle\psi^\lambda_{11}|\delta^3(\vec{r}_{12})|\psi^\lambda_{11}\rangle. \quad \text{(A5)}$$

Note that in obtaining (A5) we have not yet assumed harmonic oscillators, but only the permutational properties of ψ^ρ,ψ^λ. We have also neglected the changes in ψ^ρ,ψ^λ induced by the different masses m,m'. In the harmonic-oscillator model this amounts to the approximation $\alpha_\rho\simeq\alpha_\lambda$. For the inclusion of these effects see Sec. III.

For harmonic-oscillator wave functions (2.7) the matrix element of the δ function can be computed easily:

$$\lim_{\alpha_\rho=\alpha_\lambda}\langle\psi^\lambda_{11}|\delta^3(\vec{r}_{12})|\psi^\lambda_{11}\rangle=\frac{\alpha^3}{(2\pi)^{3/2}}. \quad \text{(A6)}$$

The matrix element of the contact term $H^{23}_{\rm cont}$ between quarks 2 and 3 is the same as that between quarks 1 and 3 since there is explicit symmetry between quarks 1 and 2 in the state $\Lambda\frac{5}{2}^-$.

TABLE III. The nontrivial matrix elements of the contact term. The entries in the table are given in units of $4\alpha_s\alpha_\rho^3/3\sqrt{2\pi}m_d^2$, also

$$y\equiv\left(\frac{2x+1}{3}\right)^{1/4}$$

and

$$f\equiv(\tfrac{3}{4}y^2+\tfrac{1}{4})^{-5/2}.$$

	$\alpha_\rho\neq\alpha_\lambda$	$\alpha_\rho=\alpha_\lambda$
$\langle\Lambda\,{}^2\lambda\|H_{\rm contact}\|\Lambda\,{}^2\lambda\rangle$	$-\frac{1}{2}$	$-\frac{1}{2}$
$\langle\Lambda\,{}^2\rho\|H_{\rm contact}\|\Lambda\,{}^2\rho\rangle$	$-\frac{1}{2}xy^2f$	$-\frac{1}{2}x$
$\langle\Lambda\,{}^2\rho\|H_{\rm contact}\|\Lambda\,{}^2\lambda\rangle$	$+\frac{1}{4}xyf$	$+\frac{1}{4}x$
$\langle\Lambda\,{}^4\rho\|H_{\rm contact}\|\Lambda\,{}^4\rho\rangle$	$+\frac{1}{4}xy^2f$	$+\frac{1}{4}x$
$\langle\Sigma\,{}^2\lambda\|H_{\rm contact}\|\Sigma\,{}^2\lambda\rangle$	$+\frac{1}{6}(1-xf)$	$+\frac{1}{6}(1-x)$
$\langle\Sigma\,{}^2\rho\|H_{\rm contact}\|\Sigma\,{}^2\rho\rangle$	0	0
$\langle\Sigma\,{}^2\rho\|H_{\rm contact}\|\Sigma\,{}^2\lambda\rangle$	$+\frac{1}{4}xyf$	$+\frac{1}{4}x$
$\langle\Sigma\,{}^4\lambda\|H_{\rm contact}\|\Sigma\,{}^4\lambda\rangle$	$+\frac{1}{4}(\frac{2}{3}+\frac{1}{3}xf)$	$+\frac{1}{4}(\frac{2}{3}+\frac{1}{3}x)$

Because the contact terms have $S=0$, $L=0$, the matrix elements derived above are also appropriate to the states $\Lambda\,{}^4\rho\frac{3}{2}^-$ and $\frac{1}{2}^-$.

One can derive similarly the matrix elements of the contact force appropriate to the configurations $^2\rho$, $^2\lambda$, and $^4\lambda$. The only difference from the previous case consists in the permutational properties of $\chi^\rho_m,\chi^\lambda_m$ (which are identical to those of $\psi^\rho_{1m},\psi^\lambda_{1m}$) and the expectation values

$$\langle\chi^\rho_m|\vec{S}_1\cdot\vec{S}_2|\chi^\rho_{m'}\rangle=-\tfrac{3}{4}\delta_{mm'} \quad \text{(A7)}$$

and

$$\langle\chi^\lambda_m|\vec{S}_1\cdot\vec{S}_2|\chi^\lambda_{m'}\rangle=\tfrac{1}{4}\delta_{mm'}. \quad \text{(A8)}$$

The results are listed in Table III, which includes also the off-diagonal matrix elements between $^2\rho$ and $^2\lambda$ states.

2. Tensor terms

Tensor terms are somewhat more intricate to compute as a result of the $S=2$, $L=2$ character of the operators involved. We shall describe in detail again only the computation of the three tensor terms (between all pairs 12, 13, 23) for the $\Lambda\frac{5}{2}^-$ state:

$$\langle\psi^\rho_{11}\chi^S_{3/2}|H^{12}_{\rm tensor}|\psi^\rho_{11}\chi^S_{3/2}\rangle\equiv\frac{2\alpha_s}{3m_d^2}\left\langle\psi^\rho_{11}\chi^S_{3/2}\left|\frac{1}{r_{12}^3}(3\vec{S}_1\cdot\hat{r}_{12}\vec{S}_2\cdot\hat{r}_{12}-\vec{S}_1\cdot\vec{S}_2)\right|\psi^\rho_{11}\chi^S_{3/2}\right\rangle \quad \text{(A9)}$$
$$=\frac{2\alpha_s}{3m_d^2}\sqrt{12}W(1,1,\tfrac{3}{2},\tfrac{3}{2};2,\tfrac{5}{2})\left\langle\psi^\rho_{11}\left\|\frac{3}{2r_{12}^3}\hat{r}_{12+}\hat{r}_{12+}\right\|\psi^\rho_{1-1}\right\rangle\left\langle\chi^S_{3/2}\left\|\frac{\sqrt{3}}{2}S_{1+}S_{2+}\right\|\chi^S_{-1/2}\right\rangle,$$

where

$$W(11,\tfrac{3}{2},\tfrac{3}{2};2,\tfrac{5}{2})=-\begin{Bmatrix}1&1&2\\ \frac{3}{2}&\frac{3}{2}&\frac{5}{2}\end{Bmatrix}=(10\sqrt{6})^{-1}$$

is a Racah coefficient[15] and the last two factors stand for the *reduced* matrix elements appropriate to the actual matrix elements displayed:

$$\left\langle \chi^S_{+1/2} \middle|\middle| \frac{\sqrt{3}}{2} S_{1+}S_{2+} \middle|\middle| \chi^S_{-3/2} \right\rangle = (\tfrac{5}{8})^{1/2}, \quad \left\langle \psi^\rho_{11} \middle|\middle| \frac{\sqrt{3}}{2} r_{12}^{-3} \hat{r}_{12+}\hat{r}_{12+} \middle|\middle| \psi^\rho_{1-1} \right\rangle = -\frac{4\alpha^3}{3\sqrt{10\pi}}, \tag{A10}$$

where the last entry is the result appropriate to harmonic oscillators in the limit $\alpha_\rho = \alpha_\lambda$. For the general case see (A3). We thus obtain

$$\langle \psi^\rho_{11}\chi^S_{3/2} | H^{12}_{\text{tensor}} | \psi^\rho_{11}\chi^S_{3/2} \rangle = (2\alpha_s/3m_d^2)(-4\alpha^3/60\sqrt{2\pi}). \tag{A11}$$

The matrix element of the tensor term in Eq. (A9) can be evaluated more directly by using the expansion

$$\vec{S}_1 \cdot \hat{r}\vec{S}_2 \cdot \hat{r} - 3^{-1}\vec{S}_1 \cdot \vec{S}_2 = (2\pi/15)^{1/2}\Big[S_{1-}S_{2-}Y_{22}(\hat{r}) - (S_{1-}S_{2z} + S_{1z}S_{2-})Y_{21}(\hat{r}) - \frac{1}{\sqrt{6}}(S_{1+}S_{2-} - 4S_{1z}S_{2z} + S_{1-}S_{2+})Y_{20}(\hat{r}) + (S_{1+}S_{2z} + S_{1z}S_{2+})Y_{2-1}(\hat{r}) + S_{1+}S_{2+}Y_{2-2}(\hat{r})\Big], \tag{A12}$$

which, however, gives rise to lengthier calculations.

The tensor force between the other pairs of quarks can be obtained from the result (A11) by making use of permutations

$$\langle \psi^\rho_{11}\chi^S_{3/2} | H^{13}_{\text{tensor}} | \psi^\rho_{11}\chi^S_{3/2} \rangle = \langle \psi^\rho_{11}\chi^S_{3/2} | H^{23}_{\text{tensor}} | \psi^\rho_{11}\chi^S_{3/2} \rangle = \langle \psi^\rho_{11}\chi^S_{3/2} | (23)(23)H^{13}_{\text{tensor}}(23)(23) | \psi^\rho_{11}\chi^S_{3/2} \rangle$$
$$= \tfrac{1}{4}x\langle \psi^\rho_{11}\chi^S_{3/2} | H^{12}_{\text{tensor}} | \psi^\rho_{11}\chi_{3/2} \rangle = \frac{x}{4}\left(\frac{2\alpha_s}{3m_d^2}\right)\left(-\frac{4\alpha^3}{60\sqrt{2\pi}}\right), \tag{A13}$$

where we have used the permutational properties (A3) and have taken into account that the expectation value of the tensor force between quarks 1 and 2 in the state ψ^λ vanishes (in the state ψ^λ the pair 12 is in an S state). Note that we have again ignored the changes in wave functions due to the different quark masses m and m'. In a similar way one can compute the other matrix elements of the tensor force in the $J = \frac{3}{2}, \frac{1}{2}$ and the off-diagonal terms $^2\rho \to {}^4\rho$, $^2\lambda \to {}^4\rho$, $^2\lambda \to {}^4\lambda$, and $^2\rho \to {}^4\lambda$. These are listed in Table IV.

3. Wave-function distortion due to $\alpha_\rho \neq \alpha_\lambda$

In calculating the hyperfine matrix elements one must in principle take into account the fact that $\alpha_\rho \neq \alpha_\lambda$ in Eq. (2.7). We have found in practice that these effects are relatively small in the $S = -1$ sector, and so do not much affect our description of this sector. Nevertheless, it is important to take these effects into account not only for accuracy and completeness, but also for the purposes of making predictions for $S = -2$, $S = -3$, and charmed sectors. The accounts of the preceding two sections were designed to allow the reader to easily check the main features of our calculation in the $S = -1$ states without becoming enmeshed in the more tedious calculations which arise when $\alpha_\rho \neq \alpha_\lambda$. Here we outline how one can take these effects into account.

The contact terms remain very easy to calculate. By replacing the arguments of the δ functions by functions of $\vec{\rho}$ and $\vec{\lambda}$ one obtains by explicit calculation the results shown in Table III.

The tensor terms are, as usual, more problematic. The matrix elements of H^{12}_{tensor} are unchanged from the values calculated in Sec. 2 of Appendix A, but to calculate the matrix elements of H^{13}_{tensor} [which are equal to those of H^{23}_{tensor} by (12) symmetry], we have made a change of variables to

$$\vec{u} \equiv \frac{\sqrt{3}}{2}\vec{\lambda} + \tfrac{1}{2}\vec{\rho} = \frac{1}{\sqrt{2}}(\vec{r}_1 - \vec{r}_3),$$

$$\vec{v} \equiv \frac{\sqrt{3}}{2}\vec{\rho} - \tfrac{1}{2}\vec{\lambda} = \frac{1}{\sqrt{6}}(\vec{r}_1 + \vec{r}_3 - 2\vec{r}_2),$$

and made use of the expansion (A12) with $\hat{r} \to \hat{u}$. After making this variable change one is left with integrations which would be straightforward were it not for a troublesome factor of

$$\exp\left[\frac{\sqrt{3}}{2}(\alpha_\lambda^2 - \alpha_\rho^2)\vec{u}\cdot\vec{v}\right]$$

appearing in the integrand. Fortunately $(\alpha_\lambda^2 - \alpha_\rho^2)$ is small here and we have found that to better than 1% accuracy in the final answer one can replace this factor by $1 + (\sqrt{3}/2)(\alpha_\lambda^2 - \alpha_\rho^2)\vec{u}\cdot\vec{v}$. The integrations may then be performed easily, the main complication being keeping track of Clebsch-Gordan coefficients. The results are shown in Table IV.

TABLE IV. The nontrivial matrix elements of the tensor term. The entries in the table are given in units of $\delta \equiv 4\alpha_s\alpha_\rho^3/3\sqrt{2\pi}\, m_d^2$ in terms of the quantities

$$g \equiv y^2(\tfrac{3}{4}y^2+\tfrac{1}{4})^{-3/2}(\tfrac{1}{4}y^2+\tfrac{3}{4})^{-1}\left(\frac{4-2y^2}{1+y^2}\right),$$

$$g' \equiv y(\tfrac{3}{4}y^2+\tfrac{1}{4})^{-3/2}(\tfrac{1}{4}y^2+\tfrac{3}{4})^{-1}\left(\frac{2}{1+y^2}\right),$$

$$h \equiv (\tfrac{3}{4}y^2+\tfrac{1}{4})^{-3/2}(\tfrac{1}{4}y^2+\tfrac{3}{4})^{-1}\left(\frac{2y^2}{1+y^2}\right),$$

$$h' \equiv (\tfrac{3}{4}y^2+\tfrac{1}{4})^{-3/2}(\tfrac{1}{4}y^2+\tfrac{3}{4})^{-1}\left(\frac{2}{1+y^2}\right),$$

where

$$y = \left(\frac{2x+1}{3}\right)^{1/4}.$$

	$\alpha_\rho \neq \alpha_\lambda$	$\alpha_\rho = \alpha_\lambda$
$\langle \Lambda\, {}^4\rho_{\frac{5}{2}}^- \lvert H_{\text{tensor}} \rvert \Lambda\, {}^4\rho_{\frac{5}{2}}^- \rangle$	$-\frac{1}{20}(\frac{2}{3}+\frac{1}{3}xg)$	$-\frac{1}{20}(\frac{2}{3}+\frac{1}{3}x)$
$\langle \Lambda\, {}^4\rho_{\frac{3}{2}}^- \lvert H_{\text{tensor}} \rvert \Lambda\, {}^4\rho_{\frac{3}{2}}^- \rangle$	$+\frac{1}{5}(\frac{2}{3}+\frac{1}{3}xg)$	$+\frac{1}{5}(\frac{2}{3}+\frac{1}{3}x)$
$\langle \Lambda\, {}^4\rho_{\frac{1}{2}}^- \lvert H_{\text{tensor}} \rvert \Lambda\, {}^4\rho_{\frac{1}{2}}^- \rangle$	$-\frac{1}{4}(\frac{2}{3}+\frac{1}{3}xg)$	$-\frac{1}{4}(\frac{2}{3}+\frac{1}{3}x)$
$\langle \Lambda\, {}^2\lambda_{\frac{3}{2}}^- \lvert H_{\text{tensor}} \rvert \Lambda\, {}^4\rho_{\frac{3}{2}}^- \rangle$	$+\frac{\sqrt{5}}{40}xg'$	$+\frac{\sqrt{5}}{40}x$
$\langle \Lambda\, {}^2\lambda_{\frac{1}{2}}^- \lvert H_{\text{tensor}} \rvert \Lambda\, {}^4\rho_{\frac{1}{2}}^- \rangle$	$-\frac{\sqrt{2}}{8}xg'$	$-\frac{\sqrt{2}}{8}x$
$\langle \Lambda\, {}^2\rho_{\frac{3}{2}}^- \lvert H_{\text{tensor}} \rvert \Lambda\, {}^4\rho_{\frac{3}{2}}^- \rangle$	$+\frac{\sqrt{5}}{40}(\frac{4}{3}-\frac{1}{3}xg)$	$+\frac{\sqrt{5}}{40}(\frac{4}{3}-\frac{1}{3}x)$
$\langle \Lambda\, {}^2\rho_{\frac{1}{2}}^- \lvert H_{\text{tensor}} \rvert \Lambda\, {}^4\rho_{\frac{1}{2}}^- \rangle$	$-\frac{\sqrt{2}}{8}(\frac{4}{3}-\frac{1}{3}xg)$	$-\frac{\sqrt{2}}{8}(\frac{4}{3}-\frac{1}{3}x)$
$\langle \Sigma\, {}^4\lambda_{\frac{5}{2}}^- \lvert H_{\text{tensor}} \rvert \Sigma\, {}^4\lambda_{\frac{5}{2}}^- \rangle$	$-\frac{1}{20}xh$	$-\frac{1}{20}x$
$\langle \Sigma\, {}^4\lambda_{\frac{3}{2}}^- \lvert H_{\text{tensor}} \rvert \Sigma\, {}^4\lambda_{\frac{3}{2}}^- \rangle$	$+\frac{1}{5}xh$	$+\frac{1}{5}x$
$\langle \Sigma\, {}^4\lambda_{\frac{1}{2}}^- \lvert H_{\text{tensor}} \rvert \Sigma\, {}^4\lambda_{\frac{1}{2}}^- \rangle$	$-\frac{1}{4}xh$	$-\frac{1}{4}x$
$\langle \Sigma\, {}^2\lambda_{\frac{3}{2}}^- \lvert H_{\text{tensor}} \rvert \Sigma\, {}^4\lambda_{\frac{3}{2}}^- \rangle$	$-\frac{\sqrt{5}}{40}xh$	$-\frac{\sqrt{5}}{40}x$
$\langle \Sigma\, {}^2\lambda_{\frac{1}{2}}^- \lvert H_{\text{tensor}} \rvert \Sigma\, {}^4\lambda_{\frac{1}{2}}^- \rangle$	$+\frac{\sqrt{2}}{8}xh$	$+\frac{\sqrt{2}}{8}x$
$\langle \Sigma\, {}^2\rho_{\frac{3}{2}}^- \lvert H_{\text{tensor}} \rvert \Sigma\, {}^4\lambda_{\frac{3}{2}}^- \rangle$	$+\frac{\sqrt{5}}{40}xh'$	$+\frac{\sqrt{5}}{40}x$
$\langle \Sigma\, {}^2\rho_{\frac{1}{2}}^- \lvert H_{\text{tensor}} \rvert \Sigma\, {}^4\lambda_{\frac{1}{2}}^- \rangle$	$-\frac{\sqrt{2}}{8}xh'$	$-\frac{\sqrt{2}}{8}x$

APPENDIX B: THE ZEROTH-ORDER MASSES

We explicitly segregate this discussion into an appendix to emphasize that the determination of the zeroth-order masses of these states is a problem quite distinct from the main concerns of this paper. The reader may, in view of this fact, wish to consider these masses to be free parameters; we would like to point out, however, that the harmonic-oscillator model can predict these masses as well, and thereby provide additional understanding of the spectrum.

In the harmonic-oscillator model we expect that the zeroth-order masses of our states will be

$$M({}^4N, {}^2N, {}^2\Delta) = m_0, \tag{B1}$$

$$M(\Lambda\,{}^2\lambda, \Sigma\,{}^2\lambda, \Sigma\,{}^4\lambda) = m_0 + \Delta m - \tfrac{5}{2}\omega\left[1-\left(\frac{2x+1}{3}\right)^{1/2}\right], \tag{B2}$$

$$M(\Lambda\,{}^2\rho, \Lambda\,{}^4\rho, \Sigma\,{}^2\rho) = m_0 + \Delta m - \tfrac{3}{2}\omega\left[1-\left(\frac{2x+1}{3}\right)^{1/2}\right], \tag{B3}$$

$$M(\Xi\,{}^2\lambda, \Xi\,{}^4\lambda) = m_0 + 2\Delta m - \omega\left[4-\tfrac{3}{2}x^{1/2}-\frac{5}{2}\left(\frac{2+x}{3}\right)^{1/2}\right], \tag{B4}$$

$$M(\Xi\,{}^2\rho) = m_0 + 2\Delta m - \omega\left[4-\tfrac{5}{2}x^{1/2}-\frac{3}{2}\left(\frac{2+x}{3}\right)^{1/2}\right], \tag{B5}$$

$$M({}^2\Omega) = m_0 + 3\Delta m - 4\omega\{1-x^{1/2}\}, \tag{B6}$$

where $\Delta m = m_s - m_d$, ω is the harmonic-oscillator spacing in the nonstrange sector, and m_0 is an unknown constant.

Within a given strangeness subspace these formulas, while specific to the harmonic-oscillator model, will be characteristic of any potential model: A heavy quark will have less energy in a given state than a lighter quark. We therefore have no doubt that this feature, which is essential to the understanding of the spectrum, is realistic. The relative positions of the $S=0$, -1, -2, and -3 sectors should also be qualitatively correct, but here, where the spacings are quite large, the uncertainties are larger than within a given strangeness sector, and it is difficult to know how much confidence to place in the predictions. To test the credibility of these formulas we have therefore turned to the ground-state baryons. We have found that with $x \simeq 0.6$, $\omega \simeq 520$ MeV, $\Delta m \simeq 280$ MeV, and [see Eqs. (A5) and (A6)]

$$\delta \equiv \frac{4\alpha_s\alpha^3}{3\sqrt{2\pi}\, m_d^2} \simeq 300 \text{ MeV} \tag{B7}$$

(where $\alpha^2 \simeq \sqrt{3Km_d}$) the analogous formulas to (B1)–(B6), coupled with the hyperfine interaction (2.1), can convincingly describe the positions of the N, Δ, Λ, Σ, Σ^*, Ξ, Ξ^*, and Ω. *We therefore use the* 56 $L=0$ *states to fix all our parameters* which then determine all of the unperturbed masses in the 70 $L=1$ states in terms of m_0. We should stress that not all our results depend, in any event, on all the parameters. For example, the mixing angles in the N^*'s are entirely independent of all parameters,[3] and the complete set of mass splittings and mixing angles in the $S=0$ sector depend

TABLE V. The matrix elements of the two-body part of the spin-orbit interaction, where

$$y \equiv \left(\frac{2x+1}{3}\right)^{1/4}, \quad P \equiv (\tfrac{3}{4}y^2+\tfrac{1}{4})^{-3/2}(\tfrac{1}{4}y^2+\tfrac{3}{4})^{-1},$$

$$Q \equiv (\tfrac{3}{4}y^2+\tfrac{1}{4})^{-3/2}(\tfrac{1}{4}y^2+\tfrac{3}{4})^{-5/2},$$

and

$$I' = Py^2\left(\frac{5-y^2}{2+2y^2}\right), \quad J' = Qy^5\left(\frac{5-y^2}{2+2y^2}\right),$$

$$I'' = P\left(\frac{3+y^2}{2+2y^2}\right), \quad J'' = Qy^3\left(\frac{3+y^2}{2+2y^2}\right),$$

$$I''' = Py\left(\frac{1+3y^2}{2+2y^2}\right), \quad J''' = Qy^4\left(\frac{1+3y^2}{2+2y^2}\right).$$

	$H^{2B}_{SO(1G)}$ $\left(\text{in units of } \delta = \frac{4\alpha_s\alpha_\rho^3}{3\sqrt{2\pi}m_d^2}\right)$	$H^{2B}_{SO(HO)}$ $\left(\text{in units of } \gamma = \frac{K}{m_d^2}\right)$
$\Lambda\,{}^4\rho\frac{5}{2}^- \to \Lambda\,{}^4\rho\frac{5}{2}^-$	$\frac{1}{2}+\frac{1}{4}\left(\frac{1+4x+x^2}{6}\right)I'$	$-\frac{1}{2}-\frac{1}{4}\left(\frac{1+x^2}{2}\right)J'$
$\Lambda\,{}^2\lambda\frac{3}{2}^- \to \Lambda\,{}^2\lambda\frac{3}{2}^-$	$\frac{3}{8}\left(\frac{x^2+2x}{3}\right)I''$	$-\frac{3}{8}x^2J''$
$\Lambda\,{}^2\rho\frac{3}{2}^- \to \Lambda\,{}^2\rho\frac{3}{2}^-$	$\frac{1}{3}+\frac{1}{24}\left(\frac{2+2x-x^2}{3}\right)I'$	$-\frac{1}{3}-\frac{1}{24}(2-x^2)J'$
$\Lambda\,{}^4\rho\frac{3}{2}^- \to \Lambda\,{}^4\rho\frac{3}{2}^-$	$-\frac{1}{3}-\frac{1}{6}\left(\frac{1+4x+x^2}{6}\right)I'$	$+\frac{1}{3}+\frac{1}{6}\left(\frac{1+x^2}{2}\right)J'$
$\Lambda\,{}^2\lambda\frac{3}{2}^- \to \Lambda\,{}^2\rho\frac{3}{2}^-$	$-\frac{1}{8}\left(\frac{1+2x}{3}\right)I'''$	$+\frac{1}{8}J'''$
$\Lambda\,{}^2\lambda\frac{3}{2}^- \to \Lambda\,{}^4\rho\frac{3}{2}^-$	$-\frac{\sqrt{5}}{8}\left(\frac{1+2x}{3}\right)I'''$	$+\frac{\sqrt{5}}{8}J'''$
$\Lambda\,{}^2\rho\frac{3}{2}^- \to \Lambda\,{}^4\rho\frac{3}{2}^-$	$-\frac{\sqrt{5}}{6}+\frac{\sqrt{5}}{24}\left(\frac{2x^2+2x-1}{3}\right)I'$	$+\frac{\sqrt{5}}{6}-\frac{\sqrt{5}}{24}(2x^2-1)J'$
$\Lambda\,{}^2\lambda\frac{1}{2}^- \to \Lambda\,{}^2\lambda\frac{1}{2}^-$	$-\frac{3}{4}\left(\frac{x^2+2x}{3}\right)I''$	$\frac{3}{4}x^2J''$
$\Lambda\,{}^2\rho\frac{1}{2}^- \to \Lambda\,{}^2\rho\frac{1}{2}^-$	$-\frac{2}{3}-\frac{1}{12}\left(\frac{2+2x-x^2}{3}\right)I'$	$\frac{2}{3}+\frac{1}{12}(2-x^2)J'$
$\Lambda\,{}^4\rho\frac{1}{2}^- \to \Lambda\,{}^4\rho\frac{1}{2}^-$	$-\frac{5}{6}-\frac{5}{12}\left(\frac{1+4x+x^2}{6}\right)I'$	$\frac{5}{6}+\frac{5}{12}\left(\frac{1+x^2}{2}\right)J'$
$\Lambda\,{}^2\lambda\frac{1}{2}^- \to \Lambda\,{}^2\rho\frac{1}{2}^-$	$\frac{1}{4}\left(\frac{1+2x}{3}\right)I'''$	$-\frac{1}{4}J'''$
$\Lambda\,{}^2\lambda\frac{1}{2}^- \to \Lambda\,{}^4\rho\frac{1}{2}^-$	$-\frac{\sqrt{2}}{8}\left(\frac{1+2x}{3}\right)I'''$	$+\frac{\sqrt{2}}{8}J'''$
$\Lambda\,{}^2\rho\frac{1}{2}^- \to \Lambda\,{}^4\rho\frac{1}{2}^-$	$-\frac{\sqrt{2}}{6}+\frac{\sqrt{2}}{24}\left(\frac{2x^2+2x-1}{3}\right)I'$	$+\frac{\sqrt{2}}{6}-\frac{\sqrt{2}}{24}(2x^2-1)J'$
$\Sigma\,{}^4\lambda\frac{5}{2}^- \to \Sigma\,{}^4\lambda\frac{5}{2}^-$	$\frac{3}{4}\left(\frac{1+4x+x^2}{6}\right)I''$	$-\frac{3}{4}\left(\frac{1+x^2}{2}\right)J''$
$\Sigma\,{}^2\lambda\frac{3}{2}^- \to \Sigma\,{}^2\lambda\frac{3}{2}^-$	$\frac{1}{8}\left(\frac{2+2x-x^2}{3}\right)I''$	$-\frac{1}{8}(2-x^2)J''$
$\Sigma\,{}^2\rho\frac{3}{2}^- \to \Sigma\,{}^2\rho\frac{3}{2}^-$	$\frac{1}{8}\left(\frac{x^2+2x}{3}\right)I'$	$-\frac{1}{8}x^2J'$

TABLE V. *(continued)*

	$H^{2B}_{SO(1G)}$ $\left(\text{in units of } \delta=\frac{4\alpha_s\alpha_\rho^3}{3\sqrt{2\pi}m_d^2}\right)$	$H^{2B}_{SO(HO)}$ $\left(\text{in units of } \gamma=\frac{K}{m_d^2}\right)$
$\Sigma\,{}^4\lambda\frac{3}{2}^- \to \Sigma\,{}^4\lambda\frac{3}{2}^-$	$-\frac{1}{2}\left(\frac{1+4x+x^2}{6}\right)I''$	$\frac{1}{2}\left(\frac{1+x^2}{2}\right)J''$
$\Sigma\,{}^2\lambda\frac{3}{2}^- \to \Sigma\,{}^2\rho\frac{3}{2}^-$	$-\frac{1}{8}\left(\frac{1+2x}{3}\right)I'''$	$\frac{1}{8}J'''$
$\Sigma\,{}^2\lambda\frac{3}{2}^- \to \Sigma\,{}^4\lambda\frac{3}{2}^-$	$\frac{\sqrt{5}}{8}\left(\frac{2x^2+2x-1}{3}\right)I''$	$-\frac{\sqrt{5}}{8}(2x^2-1)J''$
$\Sigma\,{}^2\rho\frac{3}{2}^- \to \Sigma\,{}^4\lambda\frac{3}{2}^-$	$-\frac{\sqrt{5}}{8}\left(\frac{1+2x}{3}\right)I'''$	$\frac{\sqrt{5}}{8}J'''$
$\Sigma\,{}^2\lambda\frac{1}{2}^- \to \Sigma\,{}^2\lambda\frac{1}{2}^-$	$-\frac{1}{4}\left(\frac{2+2x-x^2}{3}\right)I''$	$+\frac{1}{4}(2-x^2)J''$
$\Sigma\,{}^2\rho\frac{1}{2}^- \to \Sigma\,{}^2\rho\frac{1}{2}^-$	$-\frac{1}{4}\left(\frac{x^2+2x}{3}\right)I'$	$\frac{1}{4}x^2J'$
$\Sigma\,{}^4\lambda\frac{1}{2}^- \to \Sigma\,{}^4\lambda\frac{1}{2}^-$	$-\frac{5}{4}\left(\frac{1+4x+x^2}{6}\right)I''$	$+\frac{5}{4}\left(\frac{1+x^2}{2}\right)J''$
$\Sigma\,{}^2\lambda\frac{1}{2}^- \to \Sigma\,{}^2\rho\frac{1}{2}^-$	$\frac{1}{4}\left(\frac{1+2x}{3}\right)I'''$	$-\frac{1}{4}J'''$
$\Sigma\,{}^2\lambda\frac{1}{2}^- \to \Sigma\,{}^4\lambda\frac{1}{2}^-$	$+\frac{\sqrt{2}}{8}\left(\frac{2x^2+2x-1}{3}\right)I''$	$-\frac{\sqrt{2}}{8}(2x^2-1)J''$
$\Sigma\,{}^2\rho\frac{1}{2}^- \to \Sigma\,{}^4\lambda\frac{1}{2}^-$	$-\frac{\sqrt{2}}{8}\left(\frac{1+2x}{3}\right)I'''$	$+\frac{\sqrt{2}}{8}J'''$

only on δ which is directly determined in terms of $(M_\Delta - M_N)$. Moreover, these values for x and ω are essentially the canonical ones; that Δm seems rather larger than its canonical value we believe to be due to the fact that wave-function effects, which we have stressed here, if not taken into account make Δm *seem* smaller. Finally, in support of the utility, if not reality[17] of these parameters, we note that one can correctly obtain m_0 itself from the unperturbed position of the nucleon. In any event, we shall simply take x, ω, Δm, and δ determined in this way and apply them to the 70 $L=1$ supermultiplet. It is in this sense that all that follows is an absolute prediction with no free parameters. On the other hand, the reader who is skeptical of this approach may, as mentioned above, simply ignore our conclusions about the relative positions *between* strangeness sectors and concentrate on the results *within* a given sector. These splittings and mixing angles are essentially independent of detailed assumptions, and should be quite reliable.

In summary: We use the values $m_0 \simeq 1610$ MeV, $x = 0.6$, $\Delta m = 280$ MeV, $\omega = 520$ MeV, and $\delta = 300$ MeV as the five parameters of this analysis. In any case our results are not sensitive to the value of x and Δm; in particular, we have also used $x = 0.7$ in conjunction with the approximate formulas ($\alpha_\rho = \alpha_\lambda$) of Tables III and IV and obtained very similar eigenvalues and eigenvectors to those listed in Table II.

APPENDIX C: SPIN-ORBIT MATRIX ELEMENTS IN THE NEGATIVE-PARITY BARYONS

The conclusions of Sec. V depend upon the explicit calculation of the matrix elements of the interactions (5.1) and (5.4) arising from one gluon exchange and the confining potential, respectively. These interactions break up into two-body and three-body interactions and are so decomposed in

TABLE VI. The matrix elements of the three-body part of the spin-orbit interaction, where

$$y \equiv \left[\frac{2x+1}{3}\right]^{1/4}, \quad \boldsymbol{R} \equiv y\left(\tfrac{3}{4}y^2+\tfrac{1}{4}\right)^{-3/2}\left(\tfrac{1}{4}y^2+\tfrac{3}{4}\right)^{-1},$$

and

$$\boldsymbol{S} \equiv y^4\left(\tfrac{3}{4}y^2+\tfrac{1}{4}\right)^{-3/2}\left(\tfrac{1}{4}y^2+\tfrac{3}{4}\right)^{-5/2}.$$

	$H^{3B}_{SO(1G)}$ (in units of $\delta \equiv \frac{4}{3\sqrt{2\pi}}\frac{\alpha_s}{m_d^2}\frac{\alpha_\rho^3}{}$)	$H^{3B}_{SO(HO)}$ (in units of $\gamma = K/m_d^2$)
$\Lambda\,{}^4\rho_{\frac{5}{2}}^- \to \Lambda\,{}^4\rho_{\frac{5}{2}}^-$	$\left(\frac{1-x^2}{24}\right)Ry$	$-\left(\frac{1-x^2}{8}\right)Sy$
$\Lambda\,{}^2\lambda_{\frac{3}{2}}^- \to \Lambda\,{}^2\lambda_{\frac{3}{2}}^-$	$-\left(\frac{2x-x^2}{24}\right)Ry^{-1}$	$-\frac{x^2}{8}Sy^{-1}$
$\Lambda\,{}^2\rho_{\frac{3}{2}}^- \to \Lambda\,{}^2\rho_{\frac{3}{2}}^-$	$-\frac{6x-x^2-2}{72}Ry$	$-\frac{2+x^2}{24}Sy$
$\Lambda\,{}^4\rho_{\frac{3}{2}}^- \to \Lambda\,{}^4\rho_{\frac{3}{2}}^-$	$-\left(\frac{1-x^2}{36}\right)Ry$	$\left(\frac{1-x^2}{12}\right)Sy$
$\Lambda\,{}^2\lambda_{\frac{3}{2}}^- \to \Lambda\,{}^2\rho_{\frac{3}{2}}^-$	$\frac{1}{36}y^{-1}+\frac{2x-1}{72}R$	$\frac{1}{12}y^{-1}+\frac{1}{24}S$
$\Lambda\,{}^2\lambda_{\frac{3}{2}}^- \to \Lambda\,{}^4\rho_{\frac{3}{2}}^-$	$\frac{\sqrt{5}}{36}y^{-1}+\frac{\sqrt{5}}{72}(2x-1)R$	$\frac{\sqrt{5}}{12}y^{-1}+\frac{\sqrt{5}}{24}S$
$\Lambda\,{}^2\rho_{\frac{3}{2}}^- \to \Lambda\,{}^4\rho_{\frac{3}{2}}^-$	$\frac{\sqrt{5}}{72}(6x-1-2x^2)Ry$	$\frac{\sqrt{5}}{24}(1+2x^2)Sy$
$\Lambda\,{}^2\lambda_{\frac{1}{2}}^- \to \Lambda\,{}^2\lambda_{\frac{1}{2}}^-$	$\left(\frac{2x-x^2}{12}\right)Ry^{-1}$	$\frac{x^2}{4}Sy^{-1}$
$\Lambda\,{}^2\rho_{\frac{1}{2}}^- \to \Lambda\,{}^2\rho_{\frac{1}{2}}^-$	$\left(\frac{6x-x^2-2}{36}\right)Ry$	$\left(\frac{2+x^2}{12}\right)Sy$
$\Lambda\,{}^4\rho_{\frac{1}{2}}^- \to \Lambda\,{}^4\rho_{\frac{1}{2}}^-$	$-\left(\frac{1-x^2}{36}\right)Ry$	$\frac{1-x^2}{12}Sy$
$\Lambda\,{}^2\lambda_{\frac{1}{2}}^- \to \Lambda\,{}^2\rho_{\frac{1}{2}}^-$	$-\frac{1}{18}y^{-1}-\left(\frac{2x-1}{36}\right)R$	$-\frac{1}{6}y^{-1}-\frac{1}{12}S$
$\Lambda\,{}^2\lambda_{\frac{1}{2}}^- \to \Lambda\,{}^4\rho_{\frac{1}{2}}^-$	$+\frac{\sqrt{2}}{36}y^{-1}+\frac{\sqrt{2}}{72}(2x-1)R$	$+\frac{\sqrt{2}}{12}y^{-1}+\frac{\sqrt{2}}{24}S$
$\Lambda\,{}^2\rho_{\frac{1}{2}}^- \to \Lambda\,{}^4\rho_{\frac{1}{2}}^-$	$+\frac{\sqrt{2}}{72}(6x-1-2x^2)Ry$	$+\frac{\sqrt{2}}{24}(1+2x^2)Sy$
$\Sigma\,{}^4\lambda_{\frac{5}{2}}^- \to \Sigma\,{}^4\lambda_{\frac{5}{2}}^-$	$-\left(\frac{1-x^2}{24}\right)Ry$	$+\left(\frac{1-x^2}{8}\right)Sy$
$\Sigma\,{}^2\lambda_{\frac{3}{2}}^- \to \Sigma\,{}^2\lambda_{\frac{3}{2}}^-$	$+\left(\frac{6x-x^2-2}{72}\right)Ry$	$+\left(\frac{2+x^2}{24}\right)Sy$
$\Sigma\,{}^2\rho_{\frac{3}{2}}^- \to \Sigma\,{}^2\rho_{\frac{3}{2}}^-$	$+\left(\frac{2x-x^2}{24}\right)Ry^{-1}$	$+\frac{x^2}{8}Sy^{-1}$
$\Sigma\,{}^4\lambda_{\frac{3}{2}}^- \to \Sigma\,{}^4\lambda_{\frac{3}{2}}^-$	$+\left(\frac{1-x^2}{36}\right)Ry$	$\left(\frac{1-x^2}{12}\right)Sy$
$\Sigma\,{}^2\lambda_{\frac{3}{2}}^- \to \Sigma\,{}^2\rho_{\frac{3}{2}}^-$	$\frac{1}{36}y^{-1}+\left(\frac{2x-1}{72}\right)R$	$\frac{1}{12}y^{-1}+\frac{1}{24}S$
$\Sigma\,{}^2\lambda_{\frac{3}{2}}^- \to \Sigma\,{}^4\lambda_{\frac{3}{2}}^-$	$-\frac{\sqrt{5}}{72}(6x-1-2x^2)Ry$	$-\frac{\sqrt{5}}{24}(1+2x^2)Sy$

TABLE VI. *(continued)*

	$H^{3B}_{SO(1G)}$ (in units of $\delta \equiv \frac{4\,\alpha_s\,\alpha_0^3}{3\sqrt{2\pi}\,m_d^2}$)	$H^{3B}_{SO(HO)}$ (in units of $\gamma = K/m_d^2$)
$\Sigma\,^2\rho\frac{3}{2}^- \to \Sigma\,^4\lambda\frac{3}{2}^-$	$\frac{\sqrt{5}}{36}y^{-1} + \frac{\sqrt{5}}{72}(2x-1)R$	$\frac{\sqrt{5}}{12}y^{-1} + \frac{\sqrt{5}}{24}S$
$\Sigma\,^2\lambda\frac{1}{2}^- \to \Sigma\,^2\lambda\frac{1}{2}^-$	$-\left(\frac{6x-x^2-2}{36}\right)Ry$	$-\left(\frac{2+x^2}{12}\right)Sy$
$\Sigma\,^2\rho\frac{1}{2}^- \to \Sigma\,^2\lambda\frac{1}{2}^-$	$-\left(\frac{2x-x^2}{12}\right)Ry^{-1}$	$-\frac{x^2}{4}Sy^{-1}$
$\Sigma\,^4\lambda\frac{1}{2}^- \to \Sigma\,^2\rho\frac{1}{2}^-$	$+\left(\frac{1-x^2}{36}\right)Ry$	$-\left(\frac{1-x^2}{12}\right)Sy$
$\Sigma\,^2\lambda\frac{1}{2}^- \to \Sigma\,^2\rho\frac{1}{2}^-$	$-\frac{1}{18}y^{-1} - \left(\frac{2x-1}{36}\right)R$	$-\frac{1}{6}y^{-1} - \frac{1}{12}S$
$\Sigma\,^2\lambda\frac{1}{2}^- \to \Sigma\,^4\lambda\frac{1}{2}^-$	$-\frac{\sqrt{2}}{72}(6x-1-2x^2)Ry$	$-\frac{\sqrt{2}}{24}(1+2x^2)Sy$
$\Sigma\,^2\rho\frac{1}{2}^- \to \Sigma\,^4\lambda\frac{1}{2}^-$	$+\frac{\sqrt{2}}{36}y^{-1} + \frac{\sqrt{2}}{72}(2x-1)R$	$+\frac{\sqrt{2}}{12}y^{-1} + \frac{\sqrt{2}}{24}S$

(5.3) and (5.6). The matrix elements of the two-body part of these interactions are easily calculated as $\vec{\rho}\times\vec{p}_\rho$ is just $\vec{L}_\rho$, the angular momentum of the ρ oscillator. This simplifies only the calculation of the two-body part of H^{12}, of course, but a transformation to the variables u and v defined in Appendix A 3 can be used to calculate matrix elements of H^{13}. The results of such a calculation are given in Table V, where the entries are accurate to order $[(\alpha_\lambda - \alpha_\rho)/(\alpha_\lambda + \alpha_\rho)]^2$. We remind the reader that, as discussed at the end of Sec. III this table is complete in the sense that the matrix elements for any negative-parity baryon may be obtained from it by a suitable choice of m and m'.

The three-body spin-orbit interactions are considerably tougher and we found it necessary to use even more effort than in the previous calculations. The transformation to the coordinates u and v for

TABLE VII. The spin-orbit matrix elements in the SU(3) limit, where $\delta \equiv 4\alpha_s\alpha^3/3\sqrt{2\pi}m_d^2$, $\gamma \equiv K/m_d^2$.

	H^{2B}_{SO}	H^{3B}_{SO}
$^4 8\,\frac{5}{2}^-$	$\frac{3}{4}(\delta-\gamma)$	0
$^2 1\,\frac{3}{2}^-$	$\frac{1}{4}(\delta-\gamma)$	$-\frac{1}{12}(\delta+3\gamma)$
$\begin{pmatrix} ^2 8\,\frac{3}{2}^- \\ ^4 8\,\frac{3}{2}^- \end{pmatrix}$	$\begin{pmatrix} \frac{1}{4} & -\frac{1}{8}\sqrt{10} \\ -\frac{1}{8}\sqrt{10} & -\frac{1}{2} \end{pmatrix}(\delta-\gamma)$	$\begin{pmatrix} 0 & \frac{1}{24}\sqrt{10} \\ \frac{1}{24}\sqrt{10} & 0 \end{pmatrix}(\delta+3\gamma)$
$^2 10\,\frac{3}{2}^-$	0	$\frac{1}{12}(\delta+3\gamma)$
$^2 1\,\frac{1}{2}^-$	$-\frac{1}{2}(\delta-\gamma)$	$\frac{1}{6}(\delta+3\gamma)$
$\begin{pmatrix} ^2 8\,\frac{1}{2}^- \\ ^4 8\,\frac{1}{2}^- \end{pmatrix}$	$\begin{pmatrix} -\frac{1}{2} & -\frac{1}{4} \\ -\frac{1}{4} & -\frac{5}{4} \end{pmatrix}(\delta-\gamma)$	$\begin{pmatrix} 0 & \frac{1}{12} \\ \frac{1}{12} & 0 \end{pmatrix}(\delta+3\gamma)$
$^2 10\,\frac{1}{2}^-$	0	$-\frac{1}{6}(\delta+3\gamma)$

calculating matrix elements of H^{13} is again very useful, but other than this we can offer no advice on how to simplify the labor involved here. The results are given in Table VI.

Since the tables are rather lengthy, it may help the reader to digest their contents to examine the matrix elements of H_{SO} in the SU(3) limit which we display in Table VII.

---

*Present address: Department of Theoretical Physics, 1 Keble Road, Oxford, England.

[1a]A. De Rújula, H. Georgi, and S. L. Glashow, Phys. Rev. D 12, 147 (1975).

[1b]T. De Grand, R. L. Jaffe, K. Johnson, and J. Kiskis, Phys. Rev. D 12, 2060 (1975).

[2]See e.g. O. W. Greenberg and C. A. Nelson, Phys. Rep. 32C, 69 (1977).

[3]N. Isgur and G. Karl, Phys. Lett. 72B, 109 (1977). We shall refer to this paper as I in the text.

[4]H. Schnitzer, Phys. Lett. 65B, 239 (1976); 69B, 477 (1977); Lai-Him Chan, *ibid.* 71B, 422 (1977).

[5]A. B. Henriques, B. H. Kellett, and R. G. Moorhouse, Phys. Lett. 64B, 85 (1976).

[6]O. W. Greenberg and M. Resnikoff, Phys. Rev. 163, 1844 (1967); D. R. Digvi and O. W. Greenberg, *ibid.* 175, 2024 (1968).

[7]R. H. Dalitz, in *Proceedings of the Triangle Meeting* (VEDA, Bratislavia, Czechoslovakia, 1975); R. Hogan, Nucl. Phys. B71, 514 (1974).

[8]W. Celmaster, Phys. Rev. D 15, 1391 (1977).

[9]D. Gromes and I. O. Stamatescu, Nucl. Phys. B112, 213 (1976); D. Gromes, *ibid.* B130, 18 (1977).

[10]A. J. G. Hey, P. J. Litchfield, and R. J. Cashmore, Nucl. Phys. B95, (1975). We refer to this paper as HLC in the text. D. Faiman and D. E. Plane, *ibid.* B50, 379 (1972). We refer to this paper as FP in the text.

[11]W. Heisenberg, Z. Phys. 39, 499 (1926); G. Breit, Phys. Rev. 36, 383 (1930); E. Fermi, Z. Phys. 60, 320 (1930).

[12]When dealing with electromagnetic splittings $m_u \neq m_d$ and there are corresponding wave-function corrections which are under investigation by one of us (N.I.).

[13]As an example of the effects of this prescription, note that if quark 3 is heavier than quarks 1 and 2 it will automatically lie nearer the center of mass with the choice (2.7).

[14]G. P. Gopal *et al.*, Nucl. Phys. B119, 362 (1977); J. K. Kim, Phys. Rev. Lett. 27, 356 (1971); A. Lea *et al.*, Nucl. Phys. B56, 77 (1973); W. Langbein and F. Wagner, *ibid.* B47, 477 (1972).

[15]D. M. Brink and G. R. Satchler, *Angular Momentum* (Oxford Univ. Press, London, England, 1962); D. A. Varshalovich, A. N. Moskalev, and V. K. Hersonskii, *Kvantovia Teoria Uglovogo Momenta* (Leningrad, 1975).

[16]R. H. Dalitz, in *Fundamentals of Quark Models*, Proceedings of the Seventeenth Scottish Universities Summer School in Physics, St. Andrews, 1976, edited by I. M. Barbour and A. T. Davies (SUSSP Publications, Edinburgh, Scotland, 1977).

[17]In particular, we do not believe that ω should be considered as more than an effective spacing parameter that includes not only the effects of the confining potential but also of any short-range forces which may be present. This could explain why the Roper resonance is so low and also why the "canonical" $\omega \simeq 500$ MeV with $m_d \simeq 350$ MeV fails to give the correct proton charge radius.

[18]The value of $\alpha_s \sim 0.9$ obtained from Eq. (B7) is not very reliable since our ω is only an effective frequency; see also Ref. 17.